



**KTH Industrial Engineering  
and Management**

# Latent Heat Thermal Energy Storage for Indoor Comfort Control

Justin Ning-Wei Chiu

Doctoral Thesis 2013

KTH School of Industrial Engineering and Management  
Division of Heat and Power Technology  
SE-100 44 STOCKHOLM

ISBN 978-91-7501-679-5

TRITA-KRV Report 13/02

ISSN 1100-7990

ISRN KTH/KRV/13/02-SE

© Justin Ning-Wei Chiu, 2013

To my family







# Abstract

Equating Earth's existence to 24 hours, we, the Homo sapiens, came about in the last four seconds. Fossil fuel came to our knowledge with mass extraction dating from the Industrial Revolution two centuries ago, in other words 4 milliseconds out of Earth's 24-hour equivalent lifetime. With the unruly use of fossil fuel based resources, global temperature increase due to anthropogenic emission is projected by the Intergovernmental Panel on Climate Change (IPCC) to increase between 2 °C and 6 °C by 2100. The expected results are unprecedented climatic phenomena, such as intense tropical cyclones, extreme heat waves, and heavy precipitation among others. Limiting climate change has become one of the most discerning issues in our highly energy dependent society.

Ever-increasing energy demand goes in hand with improved living standard due to technologic and economic progress. Behavioral change is one of the ultimate solutions to reduce energy demand through adequate life style change; however such approach requires societal paradigm shift. In this thesis, we look into using energy storage technology to peak shave and to load shift energy so as to attain increased renewable energy source utilization, improved system's energy efficiency, and reduced Greenhouse Gas (GHG) emission without compromising living comfort.

High energy density thermal energy storage (TES) systems utilize phase change materials as storage mediums where thermal energy is principally stored in the form of latent heat (LH). Advantages of such systems are compact components and small storage temperature swing. However challenges remain in implementing LHTES to the built environment, namely lack of understanding of system dynamics, uncertainty in component design, and non-documented material property are to be addressed.

The goal of this thesis is to address the issues on material property characterization, on component heat transfer study and on system integration. A methodology in measuring material's thermo physical property through T-History setup is defined. Caveats of existing methodology are presented and improvements are proposed. The second part of this thesis consists of establishing valid numerical models of LHTES component for both shape stabilized and free flowing PCMs. Experimental verifications were performed and models were validated. Improvement to the thermal power performance was studied and was reached with multistage multi-PCM

storage design. Techno-economic optimization and parametric study were carried out for transient TES integrated system study. Finally, an estimation of the Swedish peak energy demand reduction was performed through study of TES implementation to the existing energy systems. The peak energy shave attained through TES implementation determines the amount of fossil fuel based marginal energy that can be reduced for a greener environment.

**Keywords:** Thermal Energy Storage; Phase Change Material; Indoor Comfort, Heat Transfer

# Sammanfattning

Om vi låter jordens livstid motsvaras av 24 timmar, har mänskligheten endast existerat under de sista fyra sekunderna. Fossila bränslen med utvinning i stor skala kom till vår kännedom under den industriella revolutionen för två sekel sedan, med andra ord fyra millisekunder av jordens dygnslånga livstid. På grund av ohämmad fossilbränsleanvändning förutspår FN:s klimatpanel (IPCC) att den av människor orsakade globala uppvärmningen blir mellan 2°C och 6°C till år 2100. Onormala klimatfenomen förväntas som resultat, till exempel starka tropiska cykloner, extrema värmeböljor, och kraftig nederbörd. Att begränsa klimatförändringarna har blivit en av de viktigaste frågorna i vårt starkt energiberöende samhälle.

Ständigt ökande efterfrågan på energi går hand i hand med förbättrad levnadsstandard på grund av teknologiska och ekonomiska framsteg under det senaste århundradet. Beteendeförändringar, att anpassa vår livsstil, har betraktats som den slutgiltiga lösningen, men en sådan strategi kräver långsiktig utbildning och vilja. I denna avhandling undersöks en ny energiteknik: energilagring, för att minska topplaster och skifta belastningen så att vi kan gå mot ett paradigmskifte i form av ökat nyttjande av förnybara energikällor, förbättrad energieffektivitet och minskade utsläpp av växthusgaser utan att ge avkall på boendekomfort.

System för termisk energilagring med hög densitet (TES) använder fasändringsmaterial som lagringsmedia, där värmeenergi huvudsakligen lagras i form av latent värme (LH). Fördelarna är kompakta komponenter och små variationer i lagringstemperatur. Utmaningar återstår i att integrera LHTES i fastigheter: bristande förståelse för systemdynamiken, osäkerhet i komponentdesign och odokumenterade materialegenskaper.

Målet med denna avhandling är att ta itu med frågor kring materialkaraktärisering, studier av värmeöverföring för komponenter och om systemintegration. En metod för att mäta materials entalpi genom Temperature-History definieras genom att identifiera brister i existerande metoder, och implementera förbättringar. Den andra aspekten består i att upprätta gångbara numeriska modellerna för LHTES, där experimentell verifiering har genomförts. Förbättring av den termiska effekten erhålls med flerstegsfasändringsmaterial-lagring. Känslighetsanalys och teknisk-ekonomisk optimering utförs för integrerad systemdesign med TES. Slutligen görs en uppskattning av hur mycket Sveriges topplast i energisystemet kan minskas

genom att studera implementering av TES. Minskningen i topplast som uppnås genom implementation av TES bestämmer mängden marginalenergi från fossila bränslen som kan reduceras för att nå ett mer uthålligt samhälle.

**Nyckelord:** Termisk energilagring; Fasändringsmaterial; Inomhuskomfort; Värmeöverföring

# Preface

This doctoral thesis is based on the PhD research work carried out in the field of thermal energy storage at the department of Energy Technology (EGI), School of Industrial Engineering and Management (ITM), Royal Institute of Technology, KTH Sweden. This work encompasses three published journal papers, and six published peer reviewed conference papers. Cold thermal energy storage overview, material property characterization, numerical modeling, experimental testing, model comparison, case study, and climate change mitigation solution are included in this work.

## Acknowledgements

I would like to express my gratitude to Mr. Conny Ryytty and the Swedish Energy Agency for providing funding for this PhD research work at KTH. Without Conny, the work would not have been possible. I would like to thank my supervisor Assoc. Prof. Viktoria Martin for leading the project while giving me freedom to explore diverse research focuses within the field of cold thermal energy storage, the mutual trust has been the basis of this work. Acknowledgement also goes to Prof. Frank Bruno and to Prof. Björn Palm for the review of this thesis. I would like to thank Prof. Luisa Cabeza for providing me valuable comments at my Licentiate Defense and her team for hosting me during my stay during the short term scientific mission, their team spirit was remarkable. I would also like to acknowledge the entire team of Energy Conservation through Energy Storage platform Annex 24 Task 42, international bonding and fruitful discussions were source of inspiration for various research work carried out through my thesis project. I would like to thank Prof. Björn Palm and Prof. Torsten Fransson for giving me the working and learning experience as KTH PhD board member and in initiating the first Erasmus Mundus PhD Program SELECT+ at KTH Energy Technology Department. Special acknowledgements go to my reference group Bengt Uusitalo, Capital Cooling; Nils Julin, Climator AB; Fredrik Setterwall, Ecostorage; Eva-Katrin Lindman, Fortum Värme AB; Stig Högnäs, Vesam AB for their expertise in the energy storage field. Thank you my friends, my families, and all of you who supported me during my studies in Sweden.

## Publications

This PhD thesis is based on the following papers. All papers are enclosed as appendices.

### Journal Publications

- I** J. NW Chiu and V. Martin. "Submerged finned heat exchanger latent heat storage design and its experimental verification". *Journal of Applied Energy*, Vol 93, pp. 507-516, 2012.

Work Input: Numerical model, Experimental work, Results analysis, and Writing of the paper.

- II** J. NW Chiu and V. Martin. "Multistage Latent Heat Cold Thermal Energy Storage Design Analysis". *Journal of Applied Energy*, in press, 10.1016/j.apenergy.2013.01.054.

Work Input: Numerical model, Results analysis, and Writing of the paper.

- III** J. NW Chiu, P. Gravoille, and V. Martin. "Active Free Cooling Optimization with Thermal Energy Storage in Stockholm". *Journal of Applied Energy*, in press, 10.1016/j.apenergy.2013.01.076.

Work Input: Sensitivity analysis, Results compilation, and Writing of the paper.

### Peer Reviewed Conference Publications

- IV** J. NW Chiu, V. Martin, and F. Setterwall. "System Integration of Latent Heat Thermal Energy Storage for Comfort Cooling Integrated in District Cooling Network". 11th International Conference on Thermal Energy Storage, Effstock, June 14-17, 2009, Stockholm, Sweden.

- V** J. NW Chiu, V. Martin, and F. Setterwall. "A Review of Thermal Energy Storage Systems with Salt Hydrate Phase Change Materials for Comfort Cooling". 11th International Conference on Thermal Energy Storage, Effstock, June 14-17, 2009, Stockholm, Sweden.

- VI** J. NW Chiu and V. Martin. "Thermal Energy Storage for Sustainable Future: Impact of Power Enhancement on Storage Performance". *Sustainable Refrigeration and Heat Pump Technology*, June 13-16, 2010, Stockholm, Sweden.

- VII** J. NW Chiu and V. Martin. "Thermal Energy Storage: Climate Change Mitigation Solution". International Conference of Sustainable Energy Storage, Feb 21-24, 2011, Belfast, Northern Ireland. [Best Paper Award.]
- VIII** P. Johansson, J. NW Chiu, and V. Martin. "Impact of Convective Heat Transfer Mechanism in Latent Heat Storage Modeling". The 12<sup>th</sup> International Conference on Thermal Energy Storage – Innos-tock, May 16-18, 2012, Lleida, Spain.

### **Publications Not Included in this Thesis**

- IX** E. Oró, J. Chiu, V. Martin, and L. F. Cabeza. "Comparative study of different numerical models of packed bed thermal energy storage systems". Applied Thermal Engineering, Vol 50, pp. 384-392, 2013.
- X** E. Oró, A. Castell, J. Chiu, V. Martin, L.F. Cabeza. "Stratification analysis in packed bed thermal energy storage systems". Journal of Applied Energy, in press, 10.1016/j.apenergy.2012.12.082.
- XI** J. NW Chiu, V. Martin and F. Setterwall. "Performance Evaluation of an Active PCM Store Using Night Time Free Cooling for Load Shifting". European Cooperation in Science and Technology, Nov 2009. Report number: 25/09, COST-STSM-TU0802-05255.
- XII** N. Athukorala, P.D. Sarathchandra, J. NW Chiu. "Feasibility Study On Absorption Cooling Based Thermal Energy Storage". International Conference in Built Environment, Dec 14-16, 2012, Kandy, Sri Lanka.
- XIII** J. NW Chiu. "Heat Transfer Aspects of Using Phase Change Material in Thermal Energy Storage Applications". Licentiate Thesis. KTH, Sweden. ISBN: 978-91-7501-034-2.

### **Contributions to the Appended Papers**

The author of this thesis is the lead author of the appended papers I to VII, where modeling, experiment, analysis and write up were performed; and the second author to paper VIII contributing with in depth data analysis and thesis work supervision. All work was done under the advice and guidance of Assoc. Prof. Viktoria Martin. Journal paper I is published, journal paper II and paper III are in press. The author's contributions to journal

---

paper I are experimental testing, numerical modeling, data analysis and writing of the paper. In journal paper II, the author performed the numerical modeling, data analysis and wrote the paper. In journal paper III, the author's contribution goes to sensitivity analysis, results compiling and paper writing. The author wrote and held oral presentations for all peer reviewed conference papers. The attended conferences were the 11<sup>th</sup> International Conference on Thermal Energy Storage- Effstock, Sweden; the International Conference on Sustainable Refrigeration and Heat Pump Technology, Sweden; the International Conference on Sustainable Energy Storage, UK; the 12<sup>th</sup> International Conference on Thermal Energy Storage- Innostock, Spain; BIT 1<sup>st</sup> Annual World Congress of Advanced Materials, China; and the 4<sup>th</sup> International Conference on Applied Energy, China.

## Thesis Outline

This thesis tackles the research topic of Thermal Energy Storage (TES) for Indoor Comfort on three levels. The thesis is divided into the following chapters with studies performed on material level, component level and system level.

**Chapter 1** states research questions and objectives of this work.

**Chapter 2** provides a comprehensive review on Latent Heat Thermal Energy Storage on material level.

**Chapter 3** presents improvements in T-History thermo physical characterization methodology.

**Chapter 4** deals with storage component design through experimental validation of numerical models. Multi-layered thermal energy storage is designed and analyzed for its thermal power rate enhancement.

**Chapter 5** investigates system level study, where system behavior with TES integration is analyzed. Techno-economic optimization of latent heat TES system using night time cooling in a passive building is performed.

**Chapter 6** devotes to assessment of TES potential as mitigating solution for Greenhouse Gas emission reduction in the Swedish energy system.

**Chapter 7** provides summary of the results obtained followed with discussion and conclusion on the raised research questions.

## Abbreviations and Nomenclature

### Symbols

$\alpha$	Thermal diffusivity	$\text{m}^2/\text{s}$
b	Temperature range parameter	-
C	Cost	€
$c_p$	Specific heat capacity	$\text{J}/(\text{K}\cdot\text{kg})$
D	Modified Dirac function	-
dt	Phase change half temperature range	K
Fo	Fourrier number	-
h	Enthalpy	$\text{J}/\text{kg}$
H	Heaviside function	-
k	Thermal conductivity	$\text{W}/(\text{m}\cdot\text{K})$
$k_n$	Constant	-
lmtd	Log mean temperature difference	K
l	Characteristic length	m
L	Latent heat	$\text{J}/\text{kg}$
LP	Learning Parameter	-
LR	Learning Rate	-
m	Mass flow rate	$\text{kg}/\text{s}$
m	Mass	kg
N	Number of payments	-
$p, \dot{Q}$	Power	W
Q	Capacity	J

r	Radius/ r-axis	m
R	Discount rate	%
$\rho$	Density	kg/m <sup>3</sup>
T	Temperature	K
$\Delta T$	Temperature difference	K
U	Overall heat transfer coefficient	W/(m <sup>2</sup> -K)
Valve	Valve opening	%
$\dot{V}$	Volume flow	m <sup>3</sup> /s
x	x-axis	m
X	Accumulated capacity	-
y	y-axis	m
z	z-axis	m

Subscripts

0	Initial	-
ambient	Outdoor ambient	-
cool	Cooling	-
in	Inlet	-
liq	Liquid	-
out	Outlet	-
max	Maximum	-
m	Melting	-
pc	Phase change	-

ref	Reference	-
room	Indoor room	-
sol	Solid	-

### Abbreviations

AC	Auxiliary Chiller	-
AFFC	Avoided fossil fuel cost	-
CTES	Cold thermal energy storage	-
GCR	Generation cost reduction	€
GHG	Greenhouse gas emission	-
FOM	Fixed operation and maintenance	€/kW
FRS	Fuel reduction share	%
HTF	Heat transfer fluid	-
LHTES	Latent heat thermal energy storage	-
PCM	Phase change material	-
PSC	Peak shaving cost	€
PSL	Peak shaved load	kWh
PSP	Peak shaved power	kW
SCW	Stratified chilled water	-
TES	Thermal energy storage	-
TESC	Thermal energy storage cost	€
VOM	Variable operation and maintenance	€/kWh

# Table of Contents

<b>ABSTRACT</b>	<b>I</b>
<b>SAMMANFATTNING</b>	<b>III</b>
<b>PREFACE</b>	<b>V</b>
ACKNOWLEDGEMENTS	V
PUBLICATIONS	VI
THESIS OUTLINE	IX
ABBREVIATIONS AND NOMENCLATURE	X
<b>TABLE OF CONTENTS</b>	<b>XIII</b>
INDEX OF FIGURES	XV
INDEX OF TABLES	XVIII
<b>1 INTRODUCTION</b>	<b>1</b>
1.1 AIM	3
1.2 MOTIVATIONS	3
1.3 OBJECTIVES	4
1.4 METHODOLOGY AND SCOPE	4
1.5 THESIS STRUCTURE	5
<b>2 REVIEW OF THERMAL ENERGY STORAGE</b>	<b>7</b>
2.1 THERMAL ENERGY STORAGE BENEFIT	7
2.2 CATEGORIZATION	8
2.3 PCM ADVANTAGES AND LIMITATIONS	12
<b>3 T-HISTORY METHOD</b>	<b>15</b>
3.1 METHOD DESCRIPTION	15
3.2 T-HISTORY MODELING AND ANALYSIS	19
3.3 IMPACT OF SETUP ORIENTATION	21
3.4 CONCLUDING REMARKS – T-HISTORY METHODOLOGY	23
<b>4 PCM STORAGE COMPONENT MODELING</b>	<b>25</b>
4.1 NUMERICAL MODELING	25
4.1.1 <i>Gelled PCM Model</i>	26
4.1.2 <i>PCM with Convection</i>	28
4.2 SALT HYDRATE BASED GELLED PCM	29
4.2.1 <i>Experimental Setup</i>	29
4.2.2 <i>Experimental Validation</i>	30
4.3 PARAFFIN BASED PCM WITH CONVECTION	32
4.3.1 <i>Modeling Results</i>	32

---

4.3.2	<i>Experimental Validation</i>	33
4.3.3	<i>Impact of Fin Spacing on Convection</i>	34
4.4	MULTISTAGE PCM POWER ENHANCEMENT	36
4.4.1	<i>Multi-PCM Concept</i>	37
4.4.2	<i>Concept Validation</i>	38
4.5	CONCLUDING REMARKS	44
<b>5</b>	<b>ACTIVE COOLING STORAGE SYSTEM INTEGRATION</b>	<b>45</b>
5.1	TES IN DISTRICT COOLING NETWORK	45
5.2	LHTES SYSTEM OPTIMIZATION	48
5.3	SENSITIVITY ANALYSIS	52
5.4	CONCLUDING REMARKS	55
<b>6</b>	<b>ENVIRONMENTAL BENEFITS OF TES</b>	<b>57</b>
6.1	OVERVIEW OF SWEDISH ENERGY USE	57
6.2	METHODOLOGY AND MODEL	58
6.3	RESULTS AND DISCUSSION ON CO <sub>2</sub> MITIGATION POTENTIAL	60
<b>7</b>	<b>CONCLUDING DISCUSSIONS</b>	<b>63</b>
7.1	CONCLUDING REMARKS	63
7.2	FUTURE WORK	66
<b>8</b>	<b>BIBLIOGRAPHY</b>	<b>69</b>

## Index of Figures

Figure 1-1 World Primary Energy Supply, adapted from (IEA, 2012)	1
Figure 1-2 Marginal Power Requirement in Sweden, adapted from (ENTSO-E, 2012)	2
Figure 2-1 Storage Strategies : Full Storage, Load Leveling and Demand Limiting, based on (Rismanchi et al., 2012)	8
Figure 2-2 Classification of Thermal Energy Storage, adapted from (Zalba et al., 2003) and (Sharma et al., 2009)	9
Figure 2-3 Commercialized Salt Hydrate Products	11
Figure 2-4 Analytical Grade Inorganic PCMs	11
Figure 3-1 T-History Schematic and Setup	16
Figure 3-2 Temperature History Curves of a PCM and a Reference Material	17
Figure 3-3 Freezing and Melting Enthalpy of Salt	20
Figure 3-4 Enthalpy of Lab Grade Paraffin Characterized with T-History Method (top) and with DSC within the Framework of Annex 24 Task 42 (bottom) (Working Group A2, 2011)	21
Figure 3-5 Lab Grade Paraffin in Vertical Setting (left) and in Horizontal Setting Position (right)	22
Figure 3-6 Solid Deposition in Melting of Paraffin	23
Figure 4-1 Meshing Grid	27
Figure 4-2 Submerged Finned Heat Exchanger	29
Figure 4-3 Temperature Measurements (left), Schematic of the Setup (right)	30
Figure 4-4 Comparison of Numerical and Experimental Results: Charging of Cold	31
Figure 4-5 Comparison of Numerical and Experimental Results: Discharging of Cold	31

Figure 4-6 Melting of PCM in One Finned Compartment (Arrows Indicate Flow Intensities)	32
Figure 4-7 Freezing of PCM during the Charging Process	33
Figure 4-8 Experimental Verification of Numerical Simulation	33
Figure 4-9 Impact of Fin Spacings on Melting Rate (taken at the 50 <sup>th</sup> min)	34
Figure 4-10 Impact of Fin Spacing on Convection (Top Left: 30 mm, Top Right: 22.5 mm, Bottom Left: 18 mm, Bottom Right: 15 mm)	35
Figure 4-11 Temperature Difference between HTF to PCM Probed at Half the Radial Distance	36
Figure 4-12 Single PCM System (top) and Multi PCM System (bottom)	37
Figure 4-13 Operating Conditions	39
Figure 4-14 TES Performance Comparison in Charging of Cold	39
Figure 4-15 PCM Temperature Profiles	40
Figure 4-16 Performance Ratio (top) and Temperature Profile in Discharge (bottom)	41
Figure 4-17 Melting and Freezing Thermal Power Comparison	42
Figure 4-18 Storage System Dynamics in Charge and Discharge	42
Figure 4-19 Temperature Profiles of PCMs at Different Layers	43
Figure 5-1 Schematics of TES Charging (continuous line) and Discharging (dashed line)	46
Figure 5-2 SCW (top) and LHTES (bottom) Cost Breakdown at Cost Break Even	48
Figure 5-3 Indoor Temperature with and without Ventilation (top) and Cooling Demand (bottom)	50
Figure 5-4 Working Modes (left to right 1: charging, 2: standby, 3: discharging)	51
Figure 5-5 Charge and Discharge Potential	51

Figure 5-6 Pareto Optimal Front	53
Figure 5-7 Comparison of Four Optimized LHTEs	54
Figure 5-8 Sensitivity Analysis of System Cost to PCM Price and Energy Tariff	54
Figure 6-1 Swedish Peak Electricity Flow (from wind, thermal power and import) in Sweden 2000-2010, adapted from (ENTSOE, 2011)	58
Figure 6-2 Heating Means (left) and Fossil Fuel Use (right) in Heating of Residential and Service Sectors	58
Figure 6-3 CO <sub>2</sub> Emission Reduction by Means of Heating	60

---

## Index of Tables

Table 1-1 Overview of the Papers Matching the Research Goals	4
Table 2-1 Advantages and Limitations of PCMs	12
Table 4-1 Heat Exchanger	29
Table 4-2 PCM Properties	38
Table 5-1 Model Input	46
Table 5-2 Cost Effective Peak Power Reduction Rate	47
Table 5-3 Model Input	49
Table 5-4 Swedish Electricity Tariff from One Major Power Company in 2010	52
Table 5-5 Coefficient of Performance	55
Table 6-1 CO <sub>2</sub> Emission by Fuel, adapted from (IEA, 2010), (Arce et al., 2011)	59
Table 6-2 Emission Tax in Sweden (currency converted to US\$) (Swedish Tax Office, 2010)	59





# 1 Introduction

Homo sapiens thrive with technologic development. As the level of living standards climbs, the need for energy also increases. In 2010, the global total primary energy supply doubled in less than 40 years, closing in to 150 PWh<sup>1</sup>, Figure 1-1. Fossil fuel based energy supply accounts for 4/5 of total yearly energy demand and contributes to around 30 Gt CO<sub>2</sub> emissions<sup>2</sup> (IEA, 2012). Anthropogenic Greenhouse Gas (GHG) emissions since the industrial revolution are very likely to cause dramatic climate change. If no measures are taken, the allowable CO<sub>2</sub> emission for 450 ppm scenario will be surpassed by 2017 causing 2 °C to 6 °C global temperature increase by the end of this century (IEA, 2012).

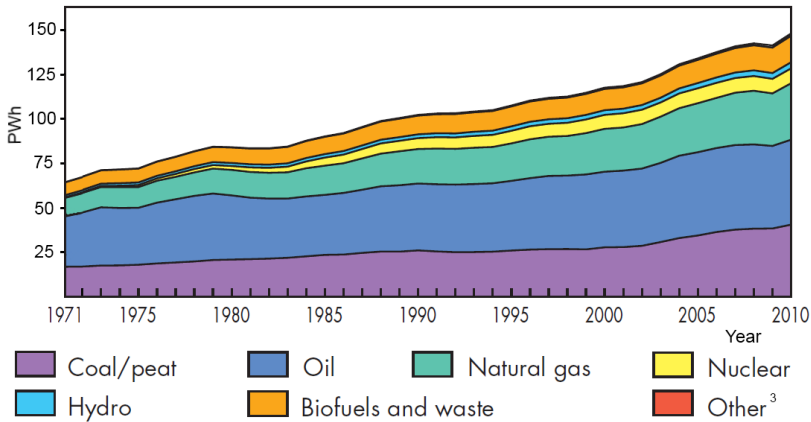


Figure 1-1 World Primary Energy Supply, adapted from (IEA, 2012)

One of the climate change mitigating technologies that have gained increasing attention is energy storage. Energy storage is one of the oldest technologies for energy conservation, it was done through ice harvesting for the purpose of food preservation (London Canal Museum, 2013). In

<sup>1</sup> 1 PWh=10<sup>3</sup> TWh

<sup>2</sup> The figure is based on combustion only

<sup>3</sup> Other renewable energies include Solar, Wind, Geothermal, etc.

the modern era, energy storage has the potential in increasing energy system efficiency and reliability through leveling of energy flow variation, namely better utilization of intermittent renewable sources and improved control on peak energy demand management. Furthermore, energy storage also contributes to load alleviation, where fossil fuel based marginal peak power production may be reduced and thus GHG emissions lowered. In Sweden, over 1 TWh/month of fossil fuel based marginal electric power production was reached during peak energy demand seasons and 1.5 TWh/month electricity was imported to meet the rising demand during winter time (ENTSO-E, 2012), Figure 1-2. Energy storage may contribute to marginal peak power production reduction.

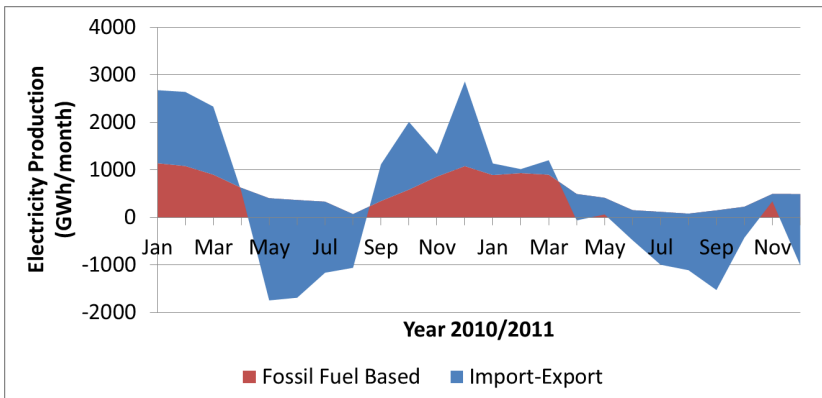


Figure 1-2 Marginal Power Requirement in Sweden, adapted from (ENTSO-E, 2012)

With the gradually sensitized population in Smart Grid concept, focus has been largely placed on Electric Energy Storage for power grid management. In parallel, heating and cooling come as more fundamental forms of energy representing a high energy share in Nordic countries. This form of energy stands for more than 45% of the total energy use in the Swedish residential and service sectors (SEA, 2011). If the heating and cooling loads are properly managed, a significant amount of marginal fossil fuel based production means may be reduced (Grozdek, 2009) (Hasnain, 2000).

Advantages of load shift and peak shave are that production units run at nominal power, attaining thus optimal operating efficiency; improved operating conditions with more suitable ambient conditions, such as running chillers during night time and heat pumps during day time; increased grid capacity without expansion expenditure; and higher use of renewable energy sources. Thermal energy storage (TES) and management is yet a field that has been much overlooked and will be the focus of this thesis. In particular, the design of TES beyond hot/cold water storage tanks is in focus here. Using so-called latent heat thermal energy

storage, or phase change materials (PCMs), the aim is to achieve storage with high energy density and the power properties needed for robust functionality.

## 1.1 Aim

This thesis is built upon the assumption that TES may be used for the benefit of the society. Relevant research questions raised in a top down approach to evaluate the statement are:

- How much can TES contribute to sustainable development and to climate change mitigation?
- What techno-economic benefits are attained in terms of energy use, infrastructure downsizing and energy management?
- What technologies and methodologies will make this happen?

With the emphasis on latent thermal energy storage for indoor comfort control, these research questions are in this thesis explored from the bottom up approach. Thus, technologies will be looked at from material study to component modeling and techno-economic analysis will be performed from system analysis to nationwide climate change mitigation assessment.

## 1.2 Motivations

In implementing storage technologies in the built environment, the design phase is one of the most crucial steps in reaching a sound and functional system. Engineers normally rely on past experience and approved methodologies in dimensioning the storage unit, provided that the storage characteristics are well documented and load profiles well defined. However, in reality, results of engineered systems often show discrepancies between the expected outcome and the real system performance. Causes are often attributed to flawed design analysis. As a matter of fact, inaccurate latent heat based TES (LHTES) understanding is often the reason behind erroneous designs. Accurate prediction of the phase change process is yet to be improved through better modeling techniques and more accurate material data input: a more in depth understanding of PCM is needed. Means for engineers to access correct PCM properties through simple but yet rigorous measurement techniques are required. Correct procedure for LHTES component design with phase change modeling is to be explored. With the above predesign requirements reached, transient behavior of a system can then be evaluated. Overall system improvement and environmental impact reduction may finally be assessed.

### 1.3 Objectives

The objective of this thesis is to establish sound procedure in designing, integrating and evaluating PCM based thermal energy storage for indoor comfort control. Through the following objectives, the research questions will be answered.

1. Demonstrate a rigorous methodology in performing material thermo-physical property (enthalpy) characterization.
2. Provide accurate numerical modeling means leading towards prediction of storage performance.
3. Display techno-economic feasibility of PCM based LHTES in system integration.
4. Determine environmental benefits with peak shaving and load shifting through use of TES.

### 1.4 Methodology and Scope

On the material-level, thermo-physical property characterizing methods such as differential scanning calorimetry (DSC) and conventional calorimetry are shown to have limitations. Therefore, the T-History method has been analyzed for its robustness in characterizing non-homogeneous materials. On the component design level, storage performance modeling has been conducted with heat transfer study based on numerical simulation methods. Heat transfer mechanisms considered in the modeling are conduction and convection, while radiation effect is negligible due to the small temperature difference. Regarding system integration, a case study of an office building on the Stockholm's district cooling network and an optimization of LHTES integrated seminar room were performed. To shed light on the environmental benefit of TES when integrated to the built environment, marginal fossil fuel based CO<sub>2</sub> emission reduction in the Swedish energy system is evaluated. Papers that contribute to reaching the aforementioned research objectives are categorized in Table 1-1.

*Table 1-1 Overview of the Papers Matching the Research Goals*

Goals	Papers
1	I, V
2	II, VIII, VI

Goals	Papers
3	III, IV
4	VII

## 1.5 Thesis Structure

The structure of this work consists of first a review on current development on thermal energy storage materials (chapter 2). Then, T-History method for material property characterization is discussed and improvements to the method are proposed (chapter 3). Assimilation of material enthalpy as a bell curve Dirac function integral is also studied and is proven to be adequate thermo physical representation of PCMs. Component modeling of heat transfer mechanism then follows; conduction only model and conduction/convection PCM model are proposed respectively to assess gelled and non-gelled PCM based LHTEs and are verified with experimental work (chapter 4). With the validated models, system study is performed; system integration optimization and sensitivity analysis are conducted (chapter 5). Finally, a preliminary evaluation on GHG emissions reduction that can be further achieved in Sweden on top of existing measures with TES is performed (chapter 6).



# 2 Review of Thermal Energy Storage

When looking for TES systems suitable to an application, the following criteria are desired: little thermal loss during storage period, high extraction efficiency of stored energy, adequate temperature, non-hazardousness to the environment, commercial availability, and cost effectiveness among others (Zalba et al., 2003) (Dincer & Rosen, 2011).

A wide range of literatures on TES have been published in recent years. This chapter provides a summary of reviews on PCM categorizations and an overview of advantages/limitations with use of PCMs. Various reviews in this field are referenced, namely (Hasnain, 1998), (Dincer, 2002), (Tyagi & Buddhi, 2007), (Agyenim et al., 2010), (Oró et al., 2012).

## 2.1 Thermal Energy Storage Benefit

TES systems are known for their contribution in an energy system through better load management (Paksoy, 2007), (Mehling & Cabeza, 2008), and (Dincer & Rosen, 2011):

- to increase generation capacity by displacing peak-period high-demand to off-peak low-demand period, and hence expend total load capacity
- to attain better operating conditions by running energy systems under the most suitable storage strategies, namely full storage, load leveling and demand limiting
- to lower energy cost with load shift from high cost periods to low cost period
- to improve system reliability with TES as a backup system

The control strategies are distinguished to full and partial displacements of the load from peak-period to off-peak period, Figure 2-1 (Rismanchi et al., 2012). The partial displacement of the load can be set to load leveling or demand limiting. In the load leveling scheme, the energy supply

is constant and the unmatched load demand is fulfilled from the storage. In the demand limiting scheme, the energy supply is lowered during peak hours, and the storage is charged at higher energy rating during off-peak hours. This control scheme is aimed at decreasing the peak energy demand, and hence the cost, in a non-uniform tariffing system.

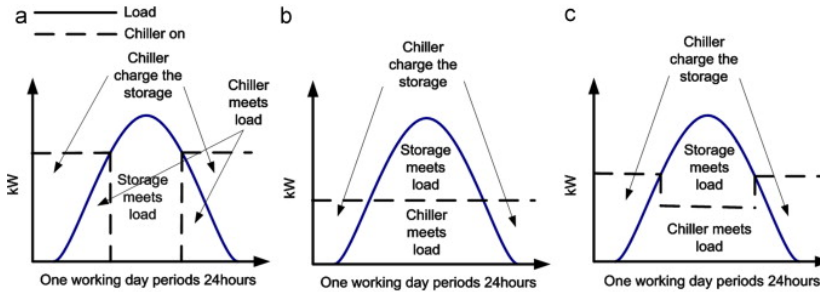


Figure 2-1 Storage Strategies: Full Storage, Load Leveling and Demand Limiting, based on (Rismanchi et al., 2012)

Economic and environmental benefits are reached with TES through downsizing of thermal and electricity producing units, operation of power generation and thermal machine at nominal capacity, utilization of off-peak-hour lower-cost energy, and reduction of marginal fossil fuel based generation.

## 2.2 Categorization

One type of categorization of TES is the division among sensible heat storage, latent heat storage and thermo chemical storage systems, Figure 2-2, adapted from (Zalba et al., 2003) and (Sharma et al., 2009).

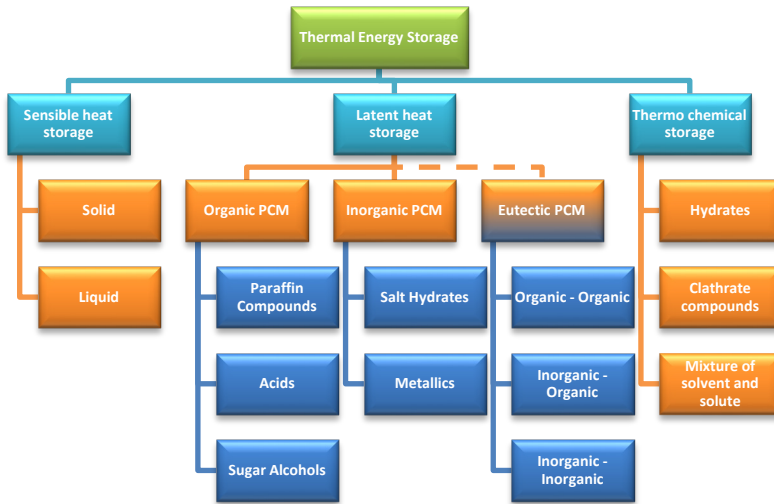


Figure 2-2 Classification of Thermal Energy Storage, adapted from (Zalba et al., 2003) and (Sharma et al., 2009)

Sensible heat storage is achieved through the change of temperature of the storage material. The amount of energy stored depends on the mass of the storage material, the specific heat capacity, and the temperature change. The stored thermal energy is expressed in Eq. 2-1.

$$Q = \int m \cdot c_p(T) \cdot dT \quad \text{Eq. 2-1}$$

where  $m$  is the mass,  $c_p(T)$  the specific heat capacity, and  $T$  the temperature.

Inherent disadvantages associated with sensible heat storage are the low storage density per degree temperature change and the large temperature range for storing the energy. Examples of sensible heat storage materials used today are liquids, such as oil, molten salt and water, e.g. in solar power plants (Medrano et al., 2010) and in chilled water storage (Rosiek & Garrido, 2012). Solid TES materials, such as rock and concrete are used for underground storage (Al-Dabbas & Al-Rousan, 2013) and in building structure (Stähl, 2009). Vapors and gases are however less utilized due to their lower volumetric storage density in comparison to liquids and solids.

Latent heat is stored through change of material phase between solid, liquid and gas. “Latent heat” refers to thermal energy storage without undergoing any temperature change, which is the situation during an ideal phase change process. The most commonly used PCMs undergo

solid-liquid phase change, for they present large heat storage density and small volume change between the two phases. Latent heat storage materials are either organics or inorganics; some also classify eutectics as a subcategory (Sharma et al., 2009), in fact they are blends of specific concentrations of either organic and/or inorganic materials. The most common organic phase change materials are paraffin and fatty acids (Farid et al., 2004) (Tyagi & Buddhi., 2007), while the most common inorganic PCMs are salt hydrates (Cabeza et al., 2011) (Al-Abidi et al., 2012). Contrary to common beliefs, most of the phase change materials undergo phase transition over a temperature range. The explanations for phase change over a certain temperature range are non-pure compounds and phase separation upon repeated freeze/melt cycles. Eutectics are compounds with specific compositions leading to sharp melting and freezing temperature without phase separation (Mehling & Cabeza, 2008).

The amount of energy that is stored over the phase change temperature range is thus the sum of the latent heat and the sensible heat over this temperature range, Eq. 2-2.

$$Q = \int_{\text{below } T_{pc}} m \cdot c_p(T) \cdot dT + \int m \cdot dh(T) + \int_{\text{above } T_{pc}} m \cdot c_p(T) \cdot dT \quad \text{Eq. 2-2}$$

where  $h$  is the phase change enthalpy and  $T_{pc}$  the phase change temperature.

The third category of TES is thermo-chemical materials based storage. As materials undergo reversible physical sorption processes and/or chemical reactions, large amount of heat is stored/released (Zalba et al., 2003). Examples of widely spread reversible thermo-chemicals are Zeolite/water, Lithium Bromide/water and Ammonium/water. The thermo-chemicals based storage systems are however more complex and their use in applications are presently being investigated (Bales, 2005).

Figure 2-3 shows a range of commercially available inorganic salt-hydrate based PCM products in the range from -40 °C to 100 °C. Ice-water transitional latent heat is plotted as a reference and is shown to be among the PCMs with the highest energy storage densities. From the data collected, it can be concluded that similar materials are used by different suppliers in the sub-zero temperature and in the indoor comfort cooling/heating range as the materials show similar latent heat. A number of analytical grade inorganic PCMs with phase change temperature between 0 °C and 40 °C are presented in Figure 2-4, where Sodium Sul-

fate Decahydrate and Calcium Chloride Hexahydrate are commonly used in this temperature range in commercialized products (Climator, 2012) (Rubitherm, 2012). By comparing latent heat of analytical grade chemicals to that of commercialized products, a significant difference in storage density is observed; this drop is due to the addition of form stabilizers, nucleating agents, and additives to stabilize mixtures from phase separation, to prevent subcooling and to control the phase change temperatures (Shin et al., 1989) (Ryu et al., 1992) (Lane, 1992).

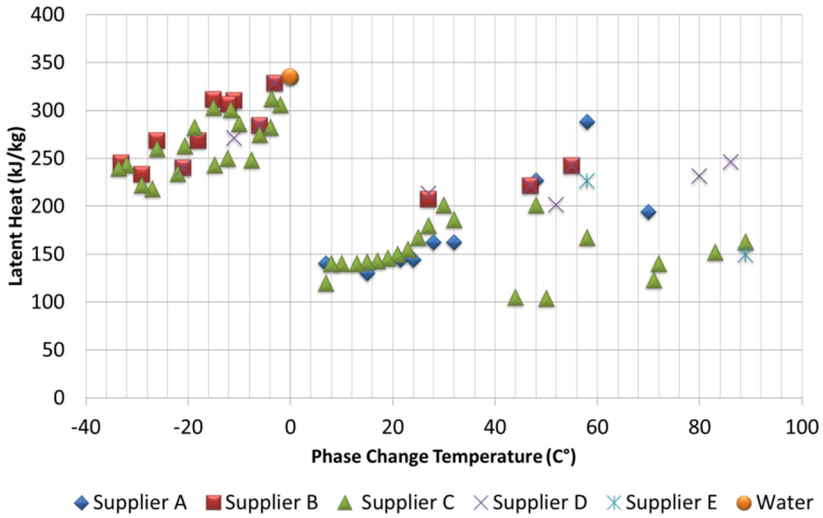


Figure 2-3 Commercialized Salt Hydrate Products

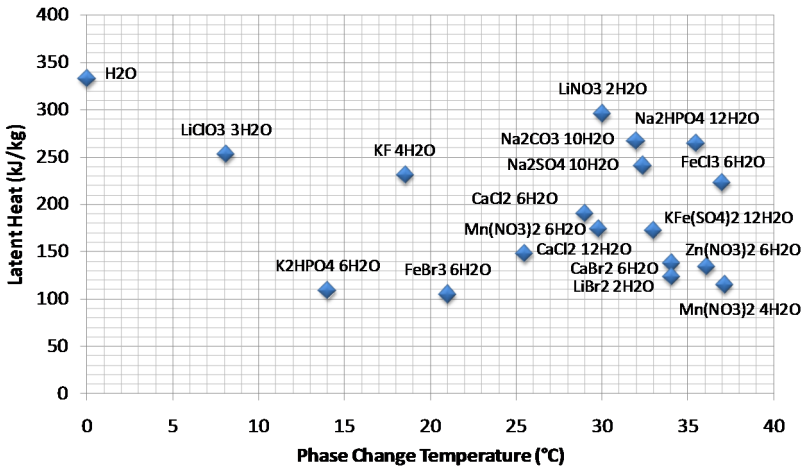


Figure 2-4 Analytical Grade Inorganic PCMs

PCMs with the following properties are highly looked after: high latent heat, small volume change, low vapor pressure, high thermal conductivity, high storage density per unit volume and per unit mass, chemical stability, non-corrosiveness, non-toxicity, non-flammability, non-segregation, self-nucleation, adequate thermal conductivity, and finally low price and abundance (Al-Abidi et al., 2012). The following section will be devoted to analyze pros and cons of latent heat storage materials.

### 2.3 PCM Advantages and Limitations

A comparison of organic and inorganic PCMs is shown in Table 2-1. Advantages of PCMs in general are their availability in a large temperature range for different working requirements, their high thermal energy storage density and quasi-constant phase change temperature. Some key characteristics of organic materials are their self-nucleating property, small subcooling, non-corrosiveness towards metallic container, and small phase segregation. Inorganic materials have generally higher thermal conductivity, hence more suitable for active TES systems; they are non-flammable, so ideal for use in buildings; and compatible with plastic containers. Eutectics are presented as a parallel category for comprehensibility; they are mixtures of organic and/or inorganic materials at specific composition providing a sharp phase change temperature.

Table 2-1 Advantages and Limitations of PCMs

	Organic	Inorganic	Eutectic
Pros	<ul style="list-style-type: none"> <li>• Self-nucleating</li> <li>• Chemically inert and stable</li> <li>• No phase segregation</li> <li>• Recyclable</li> <li>• Available in large temperature range</li> </ul>	<ul style="list-style-type: none"> <li>• High volumetric storage density (180-300 MJ/m<sup>3</sup>)</li> <li>• Higher thermal conductivity (0.7 W/m.K)</li> <li>• Non flammable</li> <li>• Low volume change</li> </ul>	<ul style="list-style-type: none"> <li>• Sharp melting point</li> <li>• High volumetric storage density</li> </ul>
Cons	<ul style="list-style-type: none"> <li>• Flammable</li> <li>• Low thermal conductivity (0.2W/m.K)</li> <li>• Low volumetric storage density (90-200 MJ/m<sup>3</sup>)</li> </ul>	<ul style="list-style-type: none"> <li>• Subcooling</li> <li>• Phase segregation</li> <li>• Corrosion of containment material</li> </ul>	<ul style="list-style-type: none"> <li>• Limited availability</li> </ul>

Adapted from (Farid et al., 2004) (White, 2005) (Sarı & Karaipekli, 2007) (Pasupathy et al., 2008) (Mehling & Cabeza, 2008) (Sharma et al., 2009) (Kuznik et al., 2011) (Cabeza et al., 2011) (Oró et al., 2012)

One major limitation of using PCMs in an active storage system is their low heat transfer performance. Although inorganic PCMs exhibit higher thermal conductivity, it rarely surpasses 0.7 W/m.K (Zalba et al., 2003) (Hauer et al., 2005). Various approaches have been taken to enhance the heat transfer rate in LHTES. Typical solutions are extension of heat transfer surface and improvement of material's thermal conductivity. The surface extension is done through the addition of fins (Ismail et al., 2001) (Castell et al., 2008) (Agyenim & Hewitt, 2010) (Tay et al., 2013), impregnation of PCM to highly conductive matrices (Mesalhy et al., 2006) (Yin et al., 2008) (Siahpush et al., 2008) (Zhao et al., 2011), insertion of high conductive fibrous materials (Frusteri et al., 2005) (Nakaso et al., 2008), and encapsulation (Regin et al., 2008) (Salunkhe & Shembekar, 2012), among others. Material property enhancement is achieved with dispersion of highly conductive particles (Wang et al., 2009) (Pincemin et al., 2008) (Oya et al., 2012). Results have shown the largest heat transfer improvement with impregnation methods reaching 130 to 180 times higher thermal conductivity (Mills et al., 2006) (Zhong et al., 2010). On the other hand, heat exchanger surface extension is a commercially mature and established method for heat transfer enhancement (Medrano et al., 2009) and will be the focus of study in this thesis.

Subcooling is yet another hindrance to the use of inorganic materials in active systems. Subcooling, sometimes also referred to as supercooling, occurs when solidification initiates below the melting temperature. Ryu (Ryu et al., 1992) reported that Sodium Sulfate Decahydrate may have subcooling reaching 20 °C below its melting point in its original form. Cold finger, which is a cold point in the storage unit, may initiate crystallization and lower the subcooling (Abhat, 1983). Nucleating agents are also used to nucleation sites to facilitate crystallization, common nucleating agents are  $\text{Na}_2\text{B}_4\text{O}_7 \cdot 10\text{H}_2\text{O}$ ,  $\text{Na}_2\text{P}_2\text{O}_7 \cdot 10\text{H}_2\text{O}$ ,  $\text{K}_2\text{SO}_4$ ,  $\text{TiO}_2$ ,  $\text{Na}_2\text{SO}_4$ ,  $\text{SrSO}_4$ ,  $\text{K}_2\text{SO}_4$ ,  $\text{SrCl}_2$ ,  $\text{BaI}_2$ ,  $\text{BaCl}_2$ ,  $\text{Ba}(\text{OH})_2$ ,  $\text{BaCO}_3$ ,  $\text{CaC}_2\text{O}_4$ ,  $\text{Sr}(\text{OH})_2$ ,  $\text{SrCO}_3$ ,  $\text{CaO}$ ,  $\text{MgSO}_4$ , and others (Farid et al., 2004) (Cabeza et al., 2011) (Li et al., 2012).

Phase segregation is the phenomenon where PCM phase-separates due to difference in density. Phase segregation can be reduced with use of gelling agents. Commonly used gelling agents are super absorbent copolymer, attapulgite clay, alginate, bentonite, starch, cellulose, and diatomaceous earth among others (Shin et al., 1989) (Ryu et al., 1992) (Cabeza et al., 2003). Artificial mixing is another solution to ensure re-mixing of the separated phases, however challenges remain in implementing the mixing and external mixing power is required (Herrick, 1982).

Other properties, such as flammability, volume change, and corrosion issues also limit the use of PCMs in building structures, and impose constraints on the storage containers as well as on the heat exchanger materials (Tyagi & Buddhi., 2007) (Sharma et al., 2009). These issues can however be overcome with adequate choice of storage container and heat exchanger material.

In thermal energy storage, one of the most eminent traits is the amount of energy that can be stored under specific working conditions. To accurately design a storage that can achieve the desired storage thermal power rate and storage capacity, correct mapping of PCM properties, especially the specific heat capacity at different temperature in melting and in freezing is needed. The following chapter 3 investigates T-History method that has gained increasing attention in material property characterization and a complete methodology of material testing to numerical representation of the property will be proposed.

## 3 T-History Method

Design of LHTES requires accurate knowledge on the thermo-physical properties of the PCMs. One of the key thermal properties is the amount of heat that can be stored in a temperature change interval, also known as enthalpy change or specific heat of capacity. Various measuring techniques, such as differential scanning calorimetry (DSC) and differential thermal analysis (DTA), are widely used for testing small sample sized homogeneous materials.

The temperature history method, also known as the T-History method, has gained wide attention when Zhang et al. (Zhang et al., 1999) showed limitation of DSC measurement for assessing properties of non-homogeneous PCM. Instead, the validity of the T-History as a method for thermo-physical property characterization was demonstrated. Various improvements to the method have then been proposed, e.g. by (Marin et al., 2003) (Hong et al., 2004) (Lázaro et al., 2006) (Günther et al., 2006) (Sandnes & Rekstad, 2006) (Peck et al., 2006) (Mehling et al., 2010) (Palomo & Dauvergne, 2011).

This section is the result of paper I and publication within the IEA Annex 24 Task 42 subgroup A2. An overview of the principle of T-History method is given in this section. In addition, this chapter presents the contribution from this dissertation in terms of improved means of conducting T-History test and a mathematical representation of the specific heat capacity is investigated.

### 3.1 Method Description

The method is based on Lumped Capacitance model where the internal temperature gradient of the measured sample is considered small. In other terms, the non-dimensional Biot number that is the ratio of the internal thermal resistance to the overall external thermal resistance should be small, Eq. 3-1.

$$Bi = \frac{U \cdot l}{k} \ll 1 \quad \text{Eq. 3-1}$$

with  $U$  the overall heat transfer coefficient accounting both the container and the insulation to the ambient,  $l$  the characteristic length of the sample, and  $k$  the thermal conductivity of the sample.

The existing methods are essentially temperature averaged models where samples are subjected to constant external ambient temperature. Here, improvements to the T-History method are proposed. The principle and calculation procedure are shown below.

Figure 3-1 shows a T-History schematic and a setup. The reference sample and the PCM sample are placed in identical containers in the temperature and humidity controlled climate chamber. Here two reference samples are utilized for double checking of the results. The lumped capacitance criterion, Eq. 3-1, is assured with well insulated containers. The climate chamber is set to vary between two temperature set points. The climate chamber temperature and the samples' temperatures are measured with PT100 sensors logged with 24 bit data acquisition system.

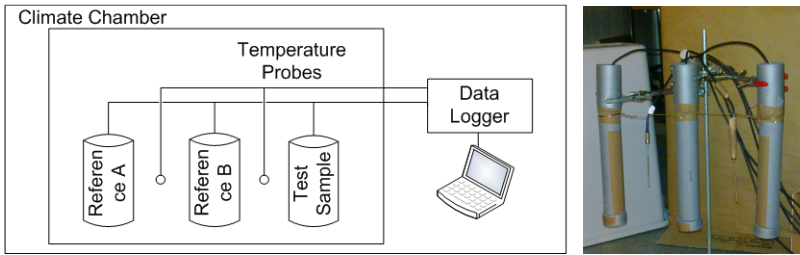


Figure 3-1 T-History Schematic and Setup

First, the internal energy change of the reference sample is evaluated with temperature change of the sample. Eq. 3-2 shows the relation between the enthalpy and the specific heat capacity.

$$\dot{Q}_{\text{ref}} = m_{\text{ref}} \Delta h_{\text{ref}} / \Delta t = m_{\text{ref}} \cdot c_{p \text{ ref}} \cdot \Delta T_{\text{ref}} / \Delta t \quad \text{Eq. 3-2}$$

where  $m$  is the mass of the sample,  $\Delta h$  is the enthalpy change,  $c_p$  is the specific heat capacity,  $T$  is the temperature and  $\Delta t$  is the time between measurements.

By considering the principle of energy conservation, the internal energy change is equal to the amount of energy transferred to the ambient, Eq. 3-3.

$$\dot{Q}_{\text{ref}} = U \cdot A_{\text{ref}} \cdot l \cdot m \cdot \Delta T \quad \text{Eq. 3-3}$$

with  $U$  the heat transfer coefficient from the climate chamber to the sample, and  $\text{lmtd}$  the logarithmic mean temperature difference, Eq. 3-4

$$\text{lmtd}_{\text{ref}} = \frac{(T_{\text{ref}}^{n-1} - T_{\text{chamber}}^{n-1}) - (T_{\text{ref}}^n - T_{\text{chamber}}^n)}{\ln\left[\frac{(T_{\text{ref}}^{n-1} - T_{\text{chamber}}^{n-1})}{(T_{\text{ref}}^n - T_{\text{chamber}}^n)}\right]} \quad \text{Eq. 3-4}$$

Here,  $T^{n-1}$  and  $T^n$  depict the sampled temperatures at times of measurement  $n-1$  and  $n$ .

Finally by combining Eq. 3-2 and Eq. 3-3, Eq. 3-5 is obtained,

$$U \cdot A_{\text{ref}} \cdot \text{lmtd} \cdot dt = m_{\text{ref}} \cdot c_{p \text{ref}} \cdot \Delta T_{\text{ref}} \quad \text{Eq. 3-5}$$

Figure 3-2 depicts an example of logged temperature history curves. The area between the climate chamber temperature and the sample temperature corresponds to the product of log mean temperature difference and the sampling time. Here,  $A$  is used for marking the area for the PCM sample and  $A'$  for the reference sample.

By replacing  $\text{lmtd} \cdot dt$  by  $A$  and  $A'$ , Eq. 3-5 can be rewritten as Eq. 3-6 for the PCM sample and as Eq. 3-7 for the reference sample,

$$U \cdot A_{\text{PCM}} \cdot A = m_{\text{PCM}} \cdot c_{p \text{PCM}} \cdot \Delta T_{\text{PCM}} \quad \text{Eq. 3-6}$$

$$U \cdot A_{\text{ref}} \cdot A' = m_{\text{ref}} \cdot c_{p \text{ref}} \cdot \Delta T_{\text{ref}} \quad \text{Eq. 3-7}$$

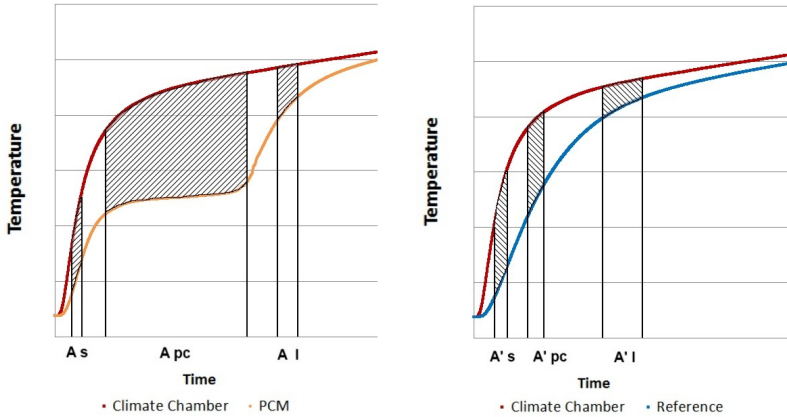


Figure 3-2 Temperature History Curves of a PCM and a Reference Material

$A_s$ ,  $A_{pc}$  and  $A_l$  mark portions of the area for the PCM sample in solid phase, during phase transition, and in liquid phase respectively, Figure 3-2 left. The areas with the same log mean temperature difference inter-

vals for the reference sample are denoted with  $A'_s$ , and  $A'_{pc}$  and  $A'_l$ , Figure 3-2 right.

As the geometries and the setups of the two samples are identical, the overall heat transfer coefficients for both samples are the same when the log mean temperature differences between the samples and the climate chamber are the same. For instance, the average overall heat transfer rate in  $A_s$ ,  $A_{pc}$ , and  $A_l$  are identical to that in  $A'_s$ ,  $A'_{pc}$ , and  $A'_l$  respectively, as the log mean temperature differences are the same in each of the three cases. It is thus possible to express the heat transfer coefficient,  $U$ , as a function of log mean temperature difference (lmtd), Eq. 3-8

$$U(\text{lmtd}) = f(\text{lmtd}) = k_1 \cdot \text{lmtd} + k_2 \quad \text{Eq. 3-8}$$

For the same log mean temperature difference,  $U$  value is identical for both the sample and the reference. The obtained  $U$  value allows verification of the Lumped capacitance criterion, Eq. 3-1.

Furthermore by combining Eq. 3-3 with Eq. 3-8, the thermal power can also be expressed as a function of lmtd,

$$\dot{Q}(\text{lmtd}) = k_3 \cdot \text{lmtd}^2 + k_4 \cdot \text{lmtd} \quad \text{Eq. 3-9}$$

The equations Eq. 3-6 and Eq. 3-7 may thus be rewritten as

$$\frac{m_{PCM} \cdot c_{p\,PCM} \cdot \Delta T_{PCM}}{A_{PCM} \cdot A} = \frac{m_{ref} \cdot c_{p\,ref} \cdot \Delta T_{ref}}{A_{ref} \cdot A'} \quad \text{Eq. 3-10}$$

As a result, the specific heat capacity may be obtained, Eq. 3-11

$$c_{p\,PCM} = \frac{m_{ref} \cdot c_{p\,ref} \cdot \Delta T_{ref}}{m_{PCM} \cdot \Delta T_{PCM}} \cdot \frac{A_{PCM} \cdot A}{A_{ref} \cdot A'} \quad \text{Eq. 3-11}$$

with

$$c_{p\,PCM} = \begin{cases} c_{p\,s} \\ c_{p\,pc} \\ c_{p\,l} \end{cases} \text{ for } A = \begin{cases} A_s \\ A_{pc} \\ A_l \end{cases} \text{ and } A' = \begin{cases} A'_s \\ A'_{pc} \\ A'_l \end{cases} \quad \text{Eq. 3-12}$$

Here, the specific heat capacity is the average value over the temperature interval of  $A$  and  $A'$ . Smaller  $A$  and  $A'$  will lead to  $c_p$  with finer temperature intervals. Further simplification to Eq. 3-11 can be made if the area for the heat exchange surface of the PCM is identical to that of the reference sample. Such an assumption is valid under the condition that the volume change of the samples is small.

In existing literature, the absolute temperature difference between ambient and the measured sample is utilized for determination of the U value e.g. (Hong et al., 2004). This limits the accuracy of results if both the chamber and the sample undergo large temperature variation. It is also proposed in literatures to have the areas  $A_s$ ,  $A_{pc}$  and  $A_l$  to cover the full range of solid phase, phase change and liquid phase, e.g., (Zhang et al., 1999) (Marin et al., 2003) (Peck et al., 2006). As a result, the material's thermo-physical property is only characterized with one general  $c_p$  value for the solid phase, one averaged latent heat value over the phase change temperature range and one  $c_p$  value for the liquid phase.

Therefore, a proposed new methodology provides further improvement to the thermo-physical results characterization on three aspects:

1. The log mean temperature difference is used for characterizing the temperature difference between the climate chamber and the samples, this provides better data analysis independently of the variation in climate chamber temperature.
2. Pose  $U=f(\text{lmt})=k_1' \cdot \text{lmt}+k_2'$  for solid phase and  $U=g(\text{lmt})=k_1'' \cdot \text{lmt}+k_2''$  for liquid phase. By injecting data obtained with the PCM sample into the curve fitted equation constants obtained from the reference sample, the uncertainty due to a single U reading is minimized.
3. The  $c_p$  determination is conducted with fixed temperature step change of the PCM (i.e. 0.1 K) so that a continuous  $c_p$  value as a function of material temperature may be obtained.

### 3.2 T-History Modeling and Analysis

A number of commercial grade PCMs and one lab grade paraffin have been tested for their enthalpy/heat capacity with the improved T-History method described above. Two test results are discussed here. The tested PCMs are denoted as Salt (a commercialized salt based PCM) and as Paraffin (98% Lab Grade Octadecane).

A numerical approximation to the measured enthalpy curve is proposed: adapted Dirac function with the form of a Gauss curve, peaking at  $T_{pc}$  and spreading over a range characterized with a temperature range parameter b. This function is described in Eq. 3-13.

$$D(T) = \frac{dH(T)}{dT} \cong \frac{e^{-\left(\frac{(T-T_{pc})^2}{b^2}\right)}}{\sqrt{\pi} \cdot b} \quad \text{Eq. 3-13}$$

The specific heat capacity is then expressed as

$$c_p(T) = H(T - T_{pc}) \cdot c_{p_{sol}} + D(T) \cdot L + H(T - T_{pc}) \cdot c_{p_{liq}} \quad Eq. 3-14$$

where  $H$  is the Heaviside function taking value of zero for negative argument and one for positive argument

and  $h$  the enthalpy expressed as in Eq. 3-15

$$h(T) = \int_{T_0}^T c_p(T) \cdot dT \quad Eq. 3-15$$

here,  $T_0$  is the reference temperature.

Figure 3-3 shows the enthalpy curve of the Salt in the range of 5 °C to 40 °C. The enthalpy obtained with the adapted Dirac approximation is also shown for comparison. The adapted Dirac approximation provides ease in performing numerical simulation in TES design. However this numerical approximation does not account for the subcooling and shows slight discrepancies in the melting process. A detailed validation of the adapted Dirac function approximation is shown in experimental verification in section 4.

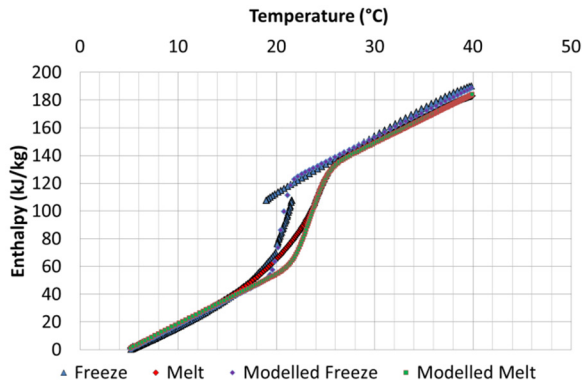


Figure 3-3 Freezing and Melting Enthalpy of Salt

Figure 3-4 (top), shows the enthalpy measurement of the Paraffin with T-History method. Within the International Energy Agency (IEA) platform Annex 24 Task 42 Energy Conservation through Energy Storage, a comparison of the obtained T-History measurement to that of DSC measurement acquired through a blind test was performed. The results show that the T-History method gives almost no hysteresis between melting and freezing curves for this PCM, while DSC demonstrates 0.5 °C to 4 °C hysteresis depending on the measurement setup, Figure 3-4

(bottom). In addition, the subcooling effect may be picked up by the T-History measurement while all DSCs do not show it.

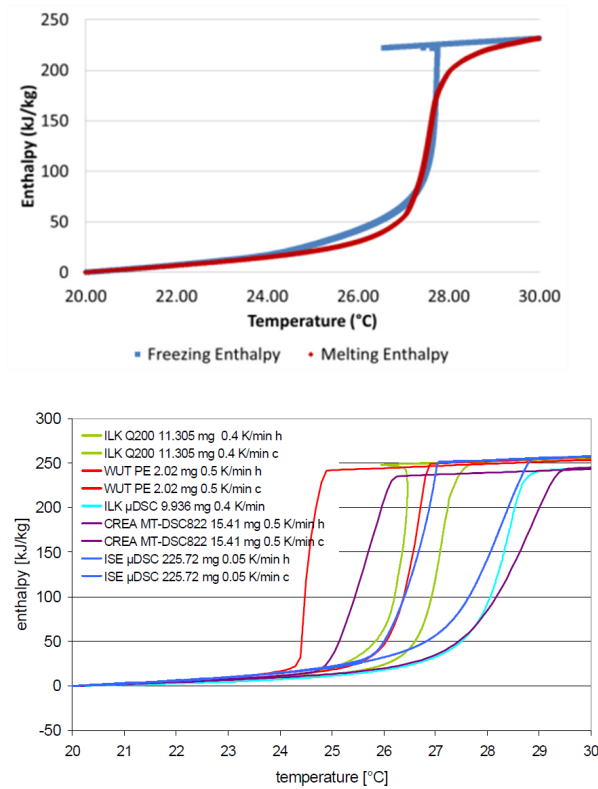


Figure 3-4 Enthalpy of Lab Grade Paraffin Characterized with T-History Method (top) and with DSC within the Framework of Annex 24 Task 42 (bottom) (Working Group A2, 2011)

One concern raised at IEA Annex 24 Task 42 platform is that the measured overall enthalpy differs between repeated measurements. This aspect will be discussed in the following section.

### 3.3 Impact of Setup Orientation

A hypothesis of solid crystals depositing to the bottom of the sample holder causing inaccurate temperature measurement was raised (Peck et al., 2006). This solid deposition and melt separation is possibly due to buoyancy in the samples. Additional vertical and horizontal T-history measurement rigs were built and the obtained thermo-physical properties were compared. The results are shown in Figure 11, with the measurements using vertical test tubes to the left, and the measurements using the horizontal test rig to the right. Here, results from the second vertically placed setup showed a higher enthalpy change over the same test-

ed temperature range, Figure 3-5 left, reaching 270 kJ/kg, as compared to the first set of results leading up to 230 kJ/kg total enthalpy change as obtained from the first vertical setup (section 3.2). The profiles of the enthalpy obtained from both vertical setups are however similar: significant discrepancies between freezing and melting enthalpy curves at the start and end of phase change.

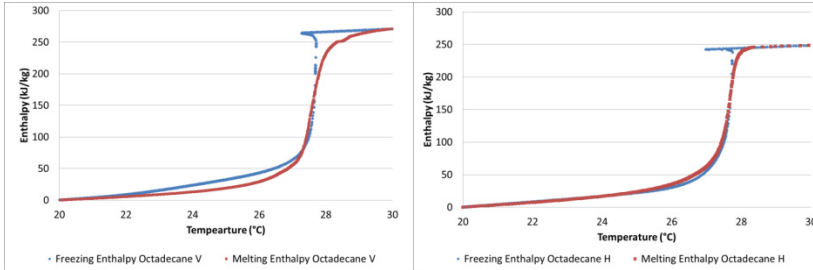
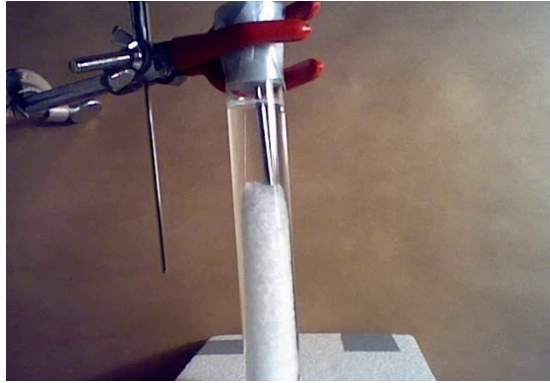


Figure 3-5 Lab Grade Paraffin in Vertical Setting (left) and in Horizontal Setting Position (right)

Enthalpy obtained with horizontal setup is shown in Figure 3-5 (right). In comparison to the vertical setup, Figure 3-5 (left), the melting and the freezing curves from the horizontal setup seem to yield measurements with a better fit in the regions where melting and freezing start; the total enthalpy change of 248 kJ/kg in the horizontal setup is also closer to the value obtained from the IEA ECES Task42 Annex24 blind test performed on DSCs among the measuring institutions, with a difference within  $\pm 3\%$ .

The over and under measurement of enthalpy in the vertical setup is explained by the fact that the deposition of the solid in the case of a non-gelled organic PCM disturbs the temperature gradient in the test sample, Figure 3-6. This temperature gradient in the test sample puts at risk the lumped capacitance assumption of uniform temperature distribution. Two outcomes are then possible in the T-history method: either the temperature sensor is placed in the upper or in the lower region of the sample container. If the temperature sensor is placed in the upper region, the measured temperature overestimates the sample temperature, causing thus an underestimation of the heat capacity. If the temperature sensor is placed in the lower region, the heat capacity will be overestimated as higher charging power is assumed to be achieved.



*Figure 3-6 Solid Deposition in Melting of Paraffin*

### 3.4 Concluding Remarks – T-history methodology

It can be concluded from this section that the T-History method is an adequate enthalpy characterization alternative to existing methods. The advantages lie on the capability of testing a larger sample size thus taking into account the non-homogeneity of the material. Cautions have to be however taken with vertical sample holders where buoyancy may influence the temperature measurement, causing either over or under estimation of the enthalpy property. The T-history method is shown here as a valid tool in characterizing material thermo-physical properties, with improvements proposed to: 1. quantify heat gain to the sample as a function of log mean temperature difference, 2. project heat transfer coefficients for solid, phase transition, and liquid phase separately, 3. perform continuous  $c_p$  measurement at fixed temperature steps with continuous heat gain function.

Future work on T-History methodology development will be focused on standardization of testing procedures, validation of consistency in repeated testing and improvement of results accuracy.



# 4 PCM Storage Component Modeling

This section is based on Paper I, "Submerged finned heat exchanger latent heat storage design and its experimental verification", Paper II, "Multistage Latent Heat Cold Thermal Energy Storage Design Analysis", and Paper VIII, "Impact of Convective Heat Transfer Mechanism in Latent Heat Storage Modeling". An effective theoretical model for PCM storage design is explained, along with the experimental verification of the model. Heat transfer aspects addressing issues on thermal power rate enhancement are proposed and discussed as well.

## 4.1 Numerical Modeling

In an active TES system where high thermal energy storage/extraction rate is needed, heat transfer in the storage material and phase change rate determine the performance of the system. Various types of numerical methods have been fine-tuned and improved to predict the behavior of a latent heat storage component. Several methods documented by researchers have evolved from one dimensional conduction based heat transfer to three dimensional models, e.g. (Voller, 1990) (Costa et al., 1998) (Wang & Yang, 2011). Three of the most revolutionizing milestones in the LH TES numerical modeling development history are:

- The enthalpy method where a single property, enthalpy, is used to predict storage capacity of the storage unit and the state of the PCM (Voller & Cross, 1981) (Teng, 1994)
- Stefan's moving front solution where the phase change border can be numerically predicted (Javierre et al., 2006) (Hinze & Ziegenbalg, 2007)
- Transformation-kinetics macro-transport models where the transport kinetics are analyzed (Verma & Mewes, 2009) (G.-Roisman et al., 2011)

These milestones are important in LHTES modeling since the employment of the enthalpy method allows determination of storage capacity with single thermal property parameter (Voller & Cross, 1981) (Teng, 1994), while Stefan's moving front solution allows prediction of melt

front of a PCM based storage (Javierre et al., 2006) (Hinze & Ziegenbalg, 2007). Finally, new approaches have been proposed to simulate heat transfer and mass transport in porous materials, such as PCM packed bed, or PCM impregnated matrices (Verma & Mewes, 2009) (G.-Roisman et al., 2011).

Here, the goal has been to develop a model to accurately predict the storage performance. A conduction only model is proposed for assessment of gelled PCM (e.g. salt hydrates), whereas a conduction/convection model is proposed for the evaluation of non-gelled PCM (e.g. paraffin).

In the conduction/convection model, the governing equations are the continuity equation, the momentum equation and the energy equation. Their formulations are presented in Eq. 4-1, Eq. 4-2, and Eq. 4-3.

$$\frac{\partial \rho}{\partial t} + \nabla \rho \mathbf{u} = 0 \quad \text{Eq. 4-1}$$

$$\rho \frac{\partial \mathbf{u}}{\partial t} + \rho \mathbf{u} \cdot \nabla \mathbf{u} = -\nabla p + \nabla \left\{ \mu [\nabla \mathbf{u} + (\nabla \mathbf{u})^T] - \frac{2}{3} \mu (\nabla \mathbf{u}) \mathbf{I} \right\} + \mathbf{F} \quad \text{Eq. 4-2}$$

$$\rho \cdot c_p \left[ \frac{\partial T}{\partial t} + (\mathbf{u} \cdot \nabla) T \right] = -(\nabla \cdot \dot{q}) + \tau S - \frac{T}{\rho} \frac{\partial \rho}{\partial T} \Big|_p \left[ \frac{\partial \rho}{\partial t} + (\mathbf{u} \cdot \nabla) \rho \right] + \dot{Q} \quad \text{Eq. 4-3}$$

In the following sections, two sets of TES models are presented. The first TES model is designed for gelled salt hydrate based storage; the second TES model is tailored for non-gelled paraffin based storage. A hypothesis for the gelled LHTES modeling is that no convective mechanism will occur due to the gelled condition, which leads to simplifications of the governing equations and lowers the required calculation power and time. Experimental verifications of both gelled and non-gelled LHTES numerical results are then carried out. Performance of non-gelled LHTES is then compared to that of gelled LHTES, and the influence of the convective heat transfer mechanism is studied.

#### 4.1.1 Gelled PCM Model

The conductive heat transfer is well established in the existing literatures, among the most prominent textbooks are (Holman, 2002) (Bird et al., 2002) (Incropera et al., 2007). One model built by the author is presented below, the tool used was Matlab. The numerical model consists of a fixed grid based mesh. The mesh grid on axial and radial plane is shown in Figure 4-1, where  $r$  is the radial direction and  $z$  the vertical direction.

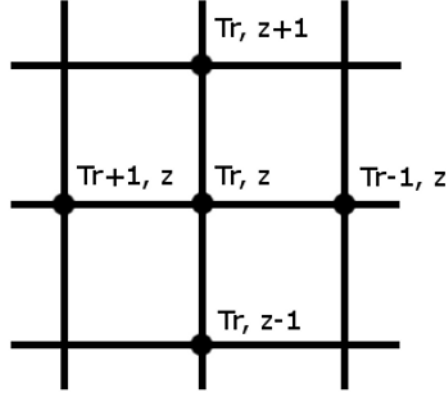


Figure 4-1 Meshing Grid

With gelled PCM, all thermal gain due to flow and viscous heating may be neglected. PCM is considered here as a non-compressible material with small volume change. Eq. 4-3 is here simplified to conduction only (shown in Eq. 4-4). Here, axial symmetry is assumed in a cylindrically shaped storage unit.

$$\frac{1}{\alpha(T)} \frac{\partial T}{\partial t} = \frac{\partial^2 T}{\partial r^2} + \frac{1}{r} \frac{\partial T}{\partial r} + \frac{\partial^2 T}{\partial z^2} \quad \text{Eq. 4-4}$$

The thermal diffusivity,  $\alpha(T)$ , is expressed in Eq. 4-5

$$\alpha(T) = \frac{k}{\rho \cdot c_p(T)} \quad \text{Eq. 4-5}$$

The discretization of the energy conservation equation performed in this model is based on an explicit finite difference scheme. The discretized equations are presented in Eq. 4-6 to Eq. 4-10.

$$\frac{\partial T}{\partial t} = \frac{T_r^{n+1} - T_r^n}{\Delta t} \quad \text{Eq. 4-6}$$

$$\frac{\partial^2 T}{\partial r^2} = \frac{T_{r+1}^n - 2T_r^n + T_{r-1}^n}{\Delta r^2} \quad \text{Eq. 4-7}$$

$$\frac{\partial T}{\partial r} = \frac{T_{r+1}^n - T_r^n}{\Delta r} \quad \text{Eq. 4-8}$$

$$\frac{\partial^2 T}{\partial z^2} = \frac{T_{z+1}^n - 2T_z^n + T_{z-1}^n}{\Delta z^2} \quad \text{Eq. 4-9}$$

$$\frac{\partial T_R^n}{\partial r} = \frac{T_R^n - T_{R-1}^n}{\Delta r} \quad \text{Eq. 4-10}$$

The convergence of the model is assured with the criterion set on the Fourier number in two-dimensional scheme, Eq. 4-11, where the ratio of the thermal diffusivity times the time step to the square of the mesh size taken in the solver has to be smaller than 0.25 to dampen error propagation (Incropera et al., 2007).

$$Fo = \frac{\alpha \cdot dt}{dr^2} < 0.25 \quad \text{Eq. 4-11}$$

The enthalpy method is based on using the enthalpy  $h(T)$  or the specific heat capacity  $c_p(T)$  to express the energy content in the storage. This allows modeling of the energy storage capacity without the need for knowing the exact position of the melting front, as a result, the simulation is simplified (Furzeland, 1980). The specific heat capacity is taken from the numerically approximated expression described in section 3.2, shown again here in Eq. 4-12.

$$c_p(T) = H(T_{pc} - T) \cdot c_{p_{sol}} + D(T) \cdot L + H(T - T_{pc}) \cdot c_{p_{liq}} \quad \text{Eq. 4-12}$$

Section 4.2 will cover the experimental verification of this numerical model with a gelled salt hydrate based PCM.

#### 4.1.2 PCM with Convection

For a non-gelled PCM, the convective mechanism must be accounted for in evaluating the heat transfer performance. To simplify the implementation of the buoyancy effect in the continuity equation and in the momentum equation, assumptions of Newtonian and incompressible fluid with isotropic properties are made, along with Boussinesq approximation. The volume force term is expressed in Eq. 4-13.

$$\mathbf{F} = \mathbf{g} \cdot \Delta \rho \quad \text{Eq. 4-13}$$

In the convection model, a computer generated non-uniform mesh grid was adapted. A mesh convergence test was performed and mesh refinement was accepted when results reach within 3% difference. The onset of fluid flow is controlled with viscosity which is a function of the temperature of the PCM. It is modeled here that convection takes place at 1 K above the peak phase change temperature in melting, and fades out at 1 K below the peak phase change temperature in freezing. A finite element based numerical software, Comsol Multiphysics v4.1 and v4.3, were used to perform the modeling. Section 4.3 is devoted to verification of this conduction/convection based model.

## 4.2 Salt Hydrate based Gelled PCM

The objective here is to verify the constructed numerical model and to determine the validity of approximating gelled LHTES to the conductive heat transfer model.

The salt hydrate based PCM was first characterized with the improved T-History method for enthalpy determination. The obtained specific heat capacity data were curve-fitted with an adapted Dirac function, and then used as input in the previously developed conduction based model. An experimental setup was built for verification of the model.

### 4.2.1 Experimental Setup

The experimental setup consists of a finned-pipe heat exchanger submerged PCM storage, Figure 4-2. The heat exchanger is made from an aluminum alloy 6082 (AL 4212) for its good thermal conductive properties and better corrosion resistance. Properties of the aluminum are given in Table 4-1.

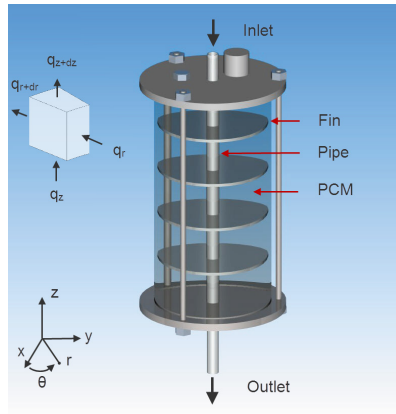


Figure 4-2 Submerged Finned Heat Exchanger

Table 4-1 Heat Exchanger

Heat Exchanger	Aluminum 6082
- Density	2700 kg/m <sup>3</sup>
- Sensible heat	894 J/kg-K
- Thermal conductivity	180 W/m-K

Temperature measurements were performed along the finned pipe, on the fins, in the PCM, and at the inlet and outlet of the heat transfer fluid (HTF), Figure 4-3 left. The fin temperature sensors were placed at 20 mm from the center of the fins, and the PCM temperature sensors were placed in the middle of the 30 mm spaced fins at the same radial distance as the fin sensors. The PCM used corresponds to the Salt presented and characterized in section 3.2. The experimental setup consists of a water bath (Lauda RA8) acting as a heat source/heat sink, a pump delivering HTF at flow rate of  $4.5 \text{ l/min} \pm 0.1 \text{ l/min}$ , a data logger (Keithley 2701, Multiplexer 7706), furthermore a 32 bit computer and type T thermocouples were also used, Figure 4-3 right.

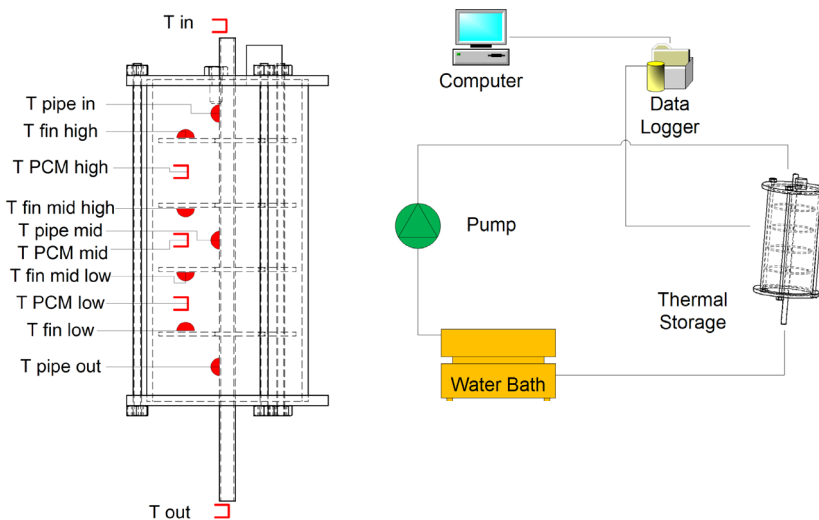


Figure 4-3 Temperature Measurements (left), Schematic of the Setup (right)

#### 4.2.2 Experimental Validation

The experimental verification were performed with charging of cold by cooling PCM from  $29 \text{ }^\circ\text{C}$  to  $15 \text{ }^\circ\text{C}$  and with discharging of cold by heating PCM from  $15 \text{ }^\circ\text{C}$  to  $29 \text{ }^\circ\text{C}$ , each process was repeated three times. The inlet HTF temperature was maintained at  $11 \text{ }^\circ\text{C}$  and  $32 \text{ }^\circ\text{C}$  respectively for charging of cold and for discharging of cold. Numerically and experimentally obtained results are shown in Figure 4-4 and Figure 4-5. The presented temperature measurements correspond to the ones probed in middle section of the test rig. For comparison, results with use of constant PCM phase change temperature are also presented.

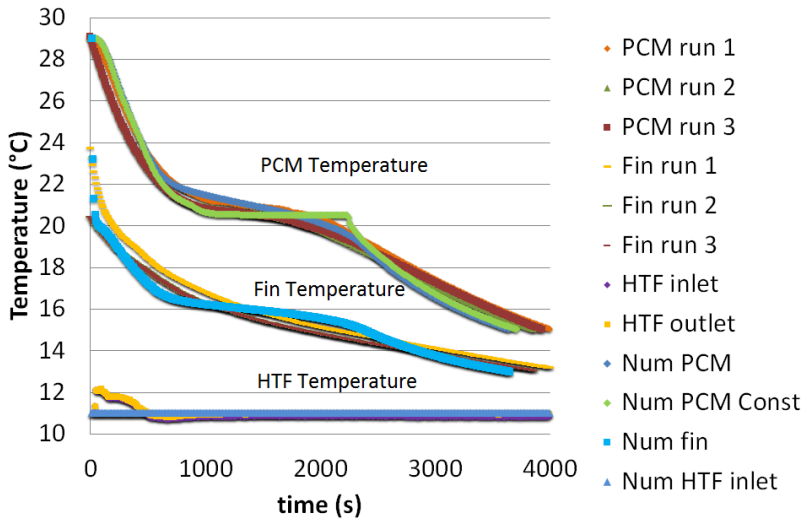


Figure 4-4 Comparison of Numerical and Experimental Results: Charging of Cold

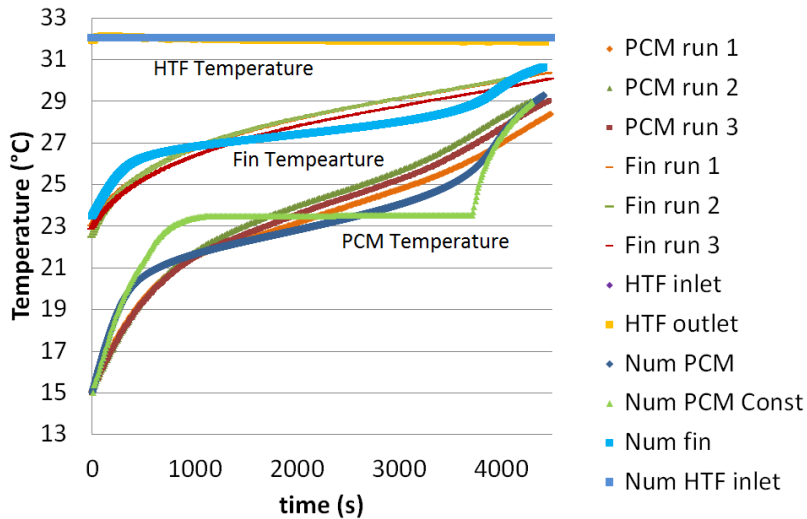


Figure 4-5 Comparison of Numerical and Experimental Results: Discharging of Cold

The proposed adapted Dirac formulation for enthalpy shows good matching in terms of temperature profiles to the experimental results. The deviations in time required to reach the same temperature are within 5%. As comparison, a large discrepancy during the phase change process is observed for the model with use of theoretical constant phase change temperature.

It can be concluded that the proposed adapted Dirac function based fixed grid finite difference model with conduction only heat transfer

mechanism is valid for evaluating performance of a gelled PCM TES giving results within 5% difference in terms of time required for reaching the same temperature. It is also shown here that the use of T-History characterized thermo-physical properties as input to the LHTES model provides more accurate results.

### 4.3 Paraffin based PCM with Convection

For a non-gelled PCM based TES, natural convection caused by buoyancy contributes to enhancement of the thermal power charge/discharge rate of the system. In this section, the effect of natural convection will be studied by comparing to a conduction only model. Experimental verification was conducted with a commercialized organic PCM (RT9) in the TES setup described previously in section 4.2.1.

#### 4.3.1 Modeling Results

Governing equations on continuity, momentum and energy conservation: Eq. 4-1, Eq. 4-2, and Eq. 4-3, constitute the base of the numerical model. The momentum equation, also known as the Navier Stokes equation, encompasses gravitational term with Boussinesq approximation.

Figure 4-6 shows the melting of PCM during the discharging process. A qualitative observation follows. The non-symmetric melt is the result of natural convection due to buoyancy. The arrows show the flow intensity of melted PCM. Natural convection is seen here emphasized along the heat exchanger pipe and in the region above the bottom fin.

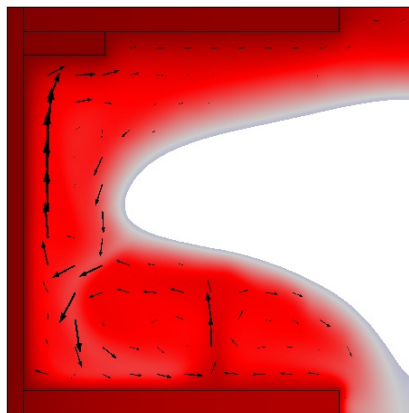


Figure 4-6 Melting of PCM in One Finned Compartment (Arrows Indicate Flow Intensities)

### 4.3.2 Experimental Validation

Freezing of RT9 paraffin based PCM in the TES unit was observed visually. Insulation was removed only for filming purpose. Figure 4-7 shows charging process at the start (left), after one hour (center), and after three hours (right).

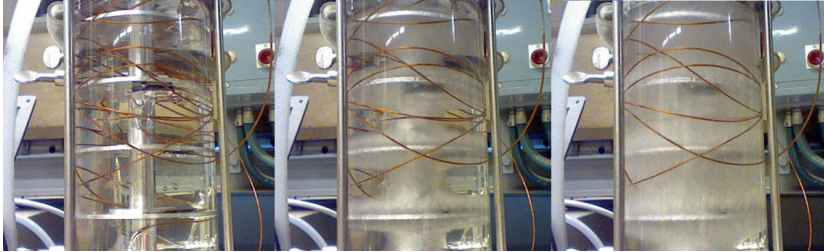


Figure 4-7 Freezing of PCM during the Charging Process

Experimental data and CFD results are shown in Figure 4-8. The positions of the simulated and the measured temperatures are identical to the ones presented in section 4.2.1. The largest discrepancy is observed when storage is in the cooler temperature solid phase. It is likely due to the discrepancy in the estimation of heat gain from the ambient. The proposed model represents adequately the physical behavior of the non-gelled PCM storage within 15% difference in terms of time required to reach the same temperature level.

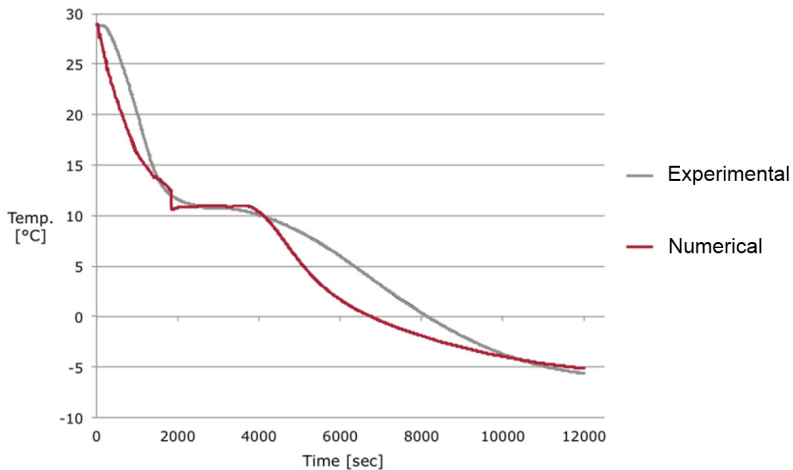


Figure 4-8 Experimental Verification of Numerical Simulation

### 4.3.3 Impact of Fin Spacing on Convection

Fin spacing has an impact on the heat exchanger surface area per storage volume. The larger the heat transfer surface area, the higher the heat exchange rate, however, a too finely placed fin configuration inhibits natural convection. Here the interdependence of effect of natural convection on finned LHTES is explored. To do so, modeling results obtained from pure conductive model and conductive/convective model on different fin configurations are compared. In this study, the initial temperature of the system was set to  $-2\text{ }^{\circ}\text{C}$  and the inner pipe temperature was considered at a constant  $30\text{ }^{\circ}\text{C}$ . Four geometric configurations were investigated, Figure 4-9, the fin spacings are: 30 mm, 22.5 mm, 18 mm and 15 mm. The simulation results at the 50<sup>th</sup> minutes are presented, the red zone indicates melt, blue region indicates the mushy zone, and the white color indicates solid.

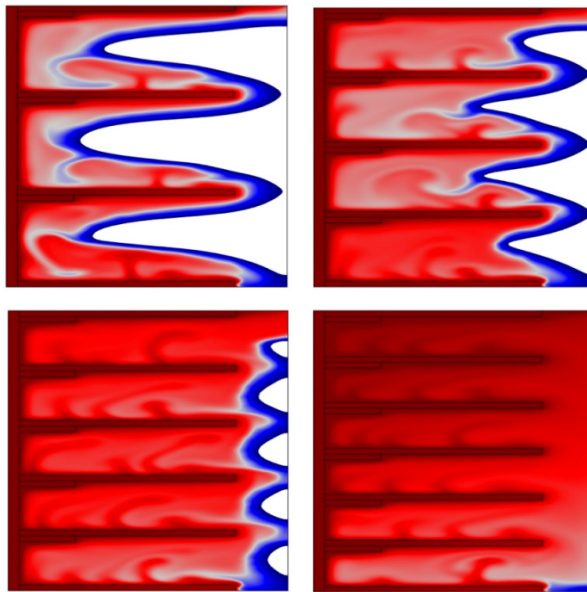


Figure 4-9 Impact of Fin Spacings on Melting Rate (taken at the 50<sup>th</sup> min)

As a general remark, finer spaced finned pipe heat exchanger leads to faster phase change, hence higher performance. Below is shown how much the convective heat transfer mechanism contributes to heat transfer in the finned geometry by comparing the gelled model to the non-gelled model.

Numerical simulations were carried out and temperature profiles of the PCM are shown in Figure 4-10. It is seen here that for fins placed less than 15 mm apart, convection has no effect on heat transfer enhancement. While for fin spacing at 18 mm, natural convection reduces the

time needed to reach 20 °C by around 5 min. For fins placed at 22.5 mm apart, the needed time is 15 min shorter. For fins placed 30 mm apart, time needed is reduced by around 30 min.

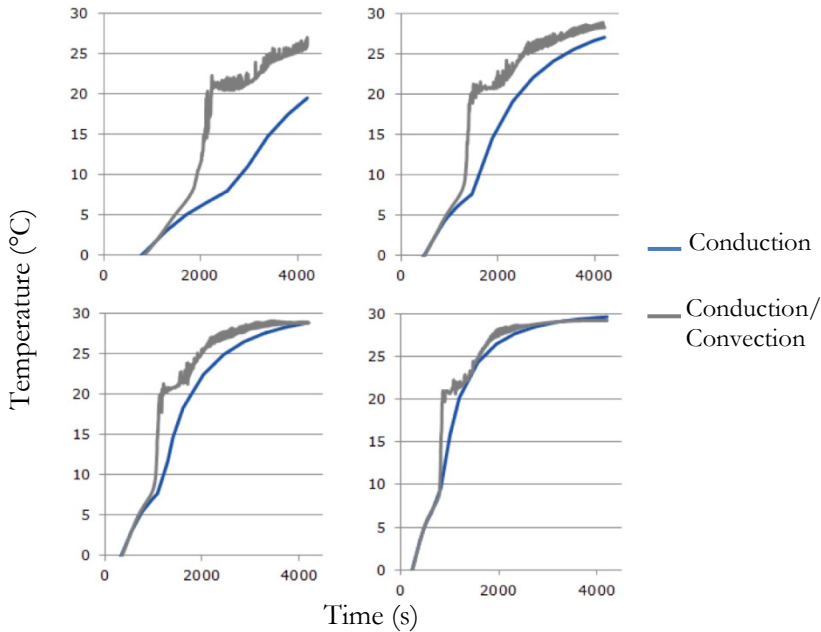


Figure 4-10 Impact of Fin Spacing on Convection (Top Left: 30 mm, Top Right: 22.5 mm, Bottom Left: 18 mm, Bottom Right: 15 mm)

Further analysis on conductive heat transfer based gelled PCM and conductive/conductive based non-gelled PCM systems were performed. The temperature differences between the HTF and the PCM at 15 mm from the pipe after 50 min and 70 min of discharging of cold are shown in Figure 4-11. A smaller temperature difference indicates a larger thermal energy capacity has been extracted/stored. This also means higher thermal power rate has been reached. The graph hence shows that finely spaced fins provide higher thermal rate. It is observed here that the difference between gelled and non-gelled temperature curves is larger at wider fin spacing, this implies that convection has a large contribution to heat transfer in systems with wider separated fins. The thermal power rate in both gelled and non-gelled LHTESs are the same when the temperature differences are at the same level. By comparing free convective PCM storage with conductive only PCM storage, non-gelled PCM with fins spaced 30 mm has similar thermal power rate as gelled PCM with fins spaced at 22.5 mm apart. The thermal power rates are identical for gelled and non-gelled PCM with fin spacing below 18 mm after 70 min and with fin spacing below 15 mm after 50 min.

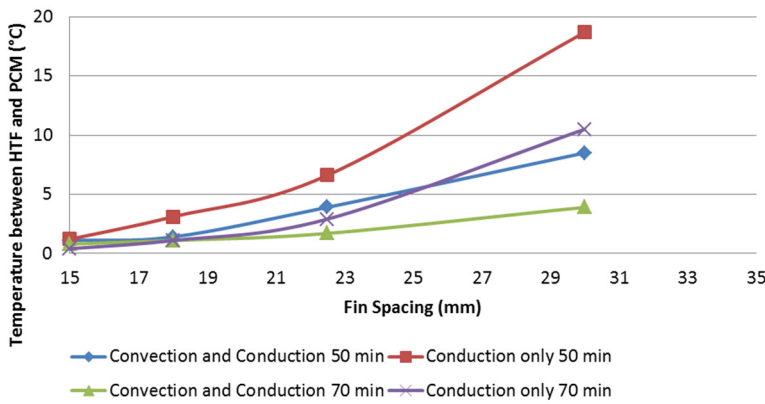


Figure 4-11 Temperature Difference between HTF to PCM Probed at Half the Radial Distance

From this study, it is shown that smaller fin spacing leads to higher thermal performance and that the convective heat transfer mechanism has a large contribution to performance enhancement for widely spread fins. On the other hand, small fin spacing leads to a reduction of convection contribution. In design of heat exchangers, this aspect needs to be considered to reach an optimal configuration in terms of low heat exchanger material cost and adequate performance level.

#### 4.4 Multistage PCM Power Enhancement

Thermal power enhancement has been a major concern in active LHTES systems where thermal power charge/extraction rate is crucial in assuring full functionality of the system. Researchers have looked into thermal power enhancement with blend of graphite brushes (Fukai et al., 2002), metallic particles (Oya et al., 2012) and foam impregnations (Almajali et al., 2013). Heat exchange surface enlargement has also been the focus of many research works, this can be achieved through encapsulation (Salunkhe & Shembekar, 2012), through addition of fins (Hosseinizadeh et al., 2011) and through direct HTF-PCM contact TES (Martin et al., 2010). Most often, only a single PCM is considered in a storage unit for energy storage purpose, a few studies have been made on multi-PCM (Gong & Mujumdar, 1996) (Shaikh & Lafdi, 2006). The multilayered PCM concept is used to maintain a constant temperature driving force throughout the storage system so as to reach higher heat transfer rate. This work proposes a comprehensive multi-PCM study with emphasize put on thermal power rate enhancement and performance quantification in both complete charge/discharge and continuous incomplete charge/discharge cycles.

#### 4.4.1 Multi-PCM Concept

The concept consists of implementing multiple PCMs with different phase change temperatures to create a more uniform temperature difference between the HTF and the PCM in the heat exchanger, enhancing thus the heat transfer rate. Figure 4-12 shows the theoretical concept of temperature profile of the HTF flowing through a single temperature PCM and that of multi-PCMs with different phase change temperatures. An analogy of the heat transfer obtained from multi-PCM system can be made to a heat exchanger placed in counter current flow, and the single PCM system to a heat exchanger placed in co-current flow. The HTF temperature in the single-PCM system is shown not being able to surpass the phase change temperature of the single-PCM, on the other hand, the HTF temperature in the multi-PCM system may reach higher temperature than that of the bottom stage and even the mid stage PCMs in the freezing process of PCMs. While reaching lower temperature than that of the top stage and the mid stage PCMs in the melting process of PCMs.

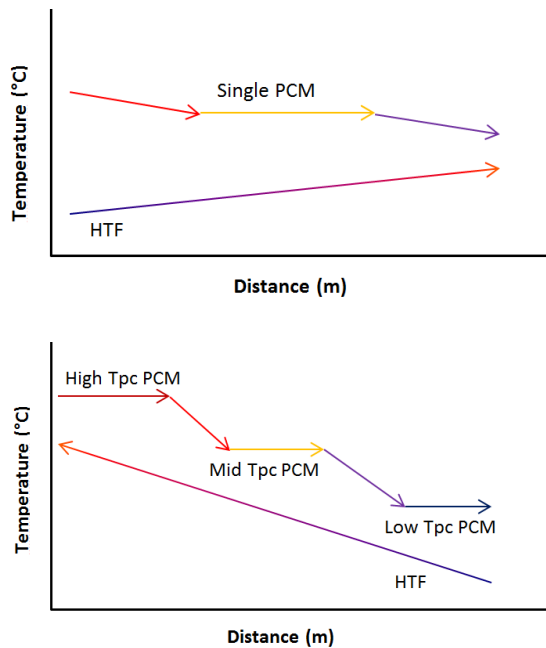


Figure 4-12 Single PCM System (top) and Multi PCM System (bottom)

The following section is devoted to concept validation of multi-PCM TES through the previously validated numerical modeling.

#### 4.4.2 Concept Validation

A study was performed to study the performance enhancement with multi-PCM TES. The same TES geometry as presented in section 4.3 was adopted for both the single-PCM and the multi-PCM storage units. The validated conduction and convection model was used. PCM peak phase change temperatures were at 7 °C, 9 °C, and 11 °C for the 3-layered PCM and the single PCM peak phase change temperature was at 9 °C. Here, PCM9 was characterized with T-History method, and the thermo-physical property was used as input for PCM 7 and for PCM 11 by shifting down the specific heat capacity by 2 °C and by shifting up the specific heat capacity by 2 °C, respectively. The PCM properties are shown in Table 4-2.

Table 4-2 PCM Properties

	PCM7	PCM9	PCM11
Peak T <sub>pc</sub>	7 °C	9 °C	11 °C
Viscosity	0.0167 Pa-s. Suppressed below T <sub>pc</sub> - 1 K during freezing and onset at T <sub>pc</sub> + 1 K during melting		
Density	800 kg/m <sup>3</sup>		
Thermal conductivity	0.2 W/m-K		
Storage capacity between 6 °C and 12 °C	Freezing: 108 kJ/kg	Freezing: 138 kJ/kg	Freezing: 149 kJ/kg
	Melting: 99 kJ/kg	Melting: 123 kJ/kg	Melting: 113 kJ/kg
Specific heat capacity	Based on c <sub>p</sub> curves measured with T-history methods		

It is observed from the PCM input parameters that the freezing capacities are 10% to 30% higher than the melting capacities. This is due to sharper freezing phase change temperature range but larger melting phase change temperature range; higher amount of latent heat is thus accounted for in the 6 °C to 12 °C working temperature range.

The operating temperature conditions for charging and discharging of the LHTES are illustrated in Figure 4-13. Charging of cold was performed with 6 °C cold inlet placed at the compartment with PCM at the lowest phase change temperature, while melting was performed with 12

°C hot inlet placed at the compartment with PCM at the highest phase change temperature.

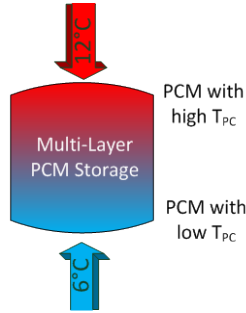


Figure 4-13 Operating Conditions

Two indicators are used to assess the thermal performance of the TES systems. The first is power ratio where the thermal power rate of the multi-PCM is compared to that of the single-PCM TES.

$$\text{Power Ratio} = \dot{Q}_{\text{multi-PCM}} / \dot{Q}_{\text{single-PCM}} \quad \text{Eq. 4-14}$$

The second is capacity ratio where stored/discharged capacity of the multi-PCM TES is compared to that of the single-PCM TES.

$$\text{Capacity Ratio} = Q_{\text{multi-PCM}} / Q_{\text{single-PCM}} \quad \text{Eq. 4-15}$$

In the process of charging cold, the power ratio achieved with the given configuration of the storage unit reaches almost 1.4 when all three layers of multi-PCM storage enter phase change process, Figure 4-14. The power ratio then drops gradually as the storage fills up. At multi-PCM capacity of 80% of its capacity, the power ratio drops below 1.

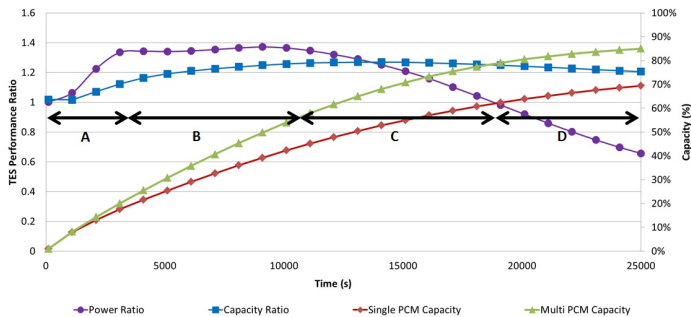


Figure 4-14 TES Performance Comparison in Charging of Cold

The PCM temperatures at each of the 3 layers are presented in Figure 4-15. Part A corresponds to the initialization of PCM layers reaching their respective phase change temperatures, hence an increase in power ratio; section B corresponds to the phase change of the three layered PCM, the power ratio is at its peak; part C corresponds to full utilization of the latent heat storage of the multi-layered PCM denoted with  $\alpha$ ,  $\beta$ , and  $\gamma$ , this is when the power ratio starts to drop; part D corresponds to multi-layered storage capacity saturating and the power ratio drops below 1.

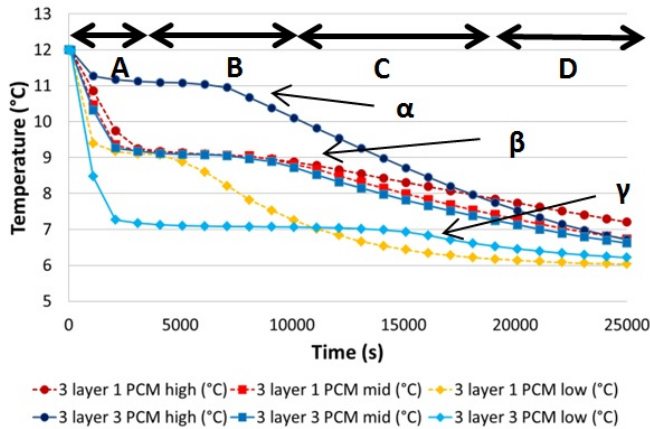


Figure 4-15 PCM Temperature Profiles

A similar trend of increase/leveling/and drop in power ratio is observed in discharging (of cold). Here, a peak power ratio of 1.1 is observed (as compared to 1.4 in the charging process). Then at 75% and 65% of full charge capacity for multi-PCM and single-PCM TESs, respectively, the power ratio drops below 1, Figure 4-16 left. The reason for the lower peak power ratio in discharging mode, as compared to charging mode, is primarily due to the larger phase change temperature range involved in the melting process, Figure 4-16 right. This large phase change temperature range results in smaller PCM to HTF temperature difference, and hence a less effective heat transfer mechanism.

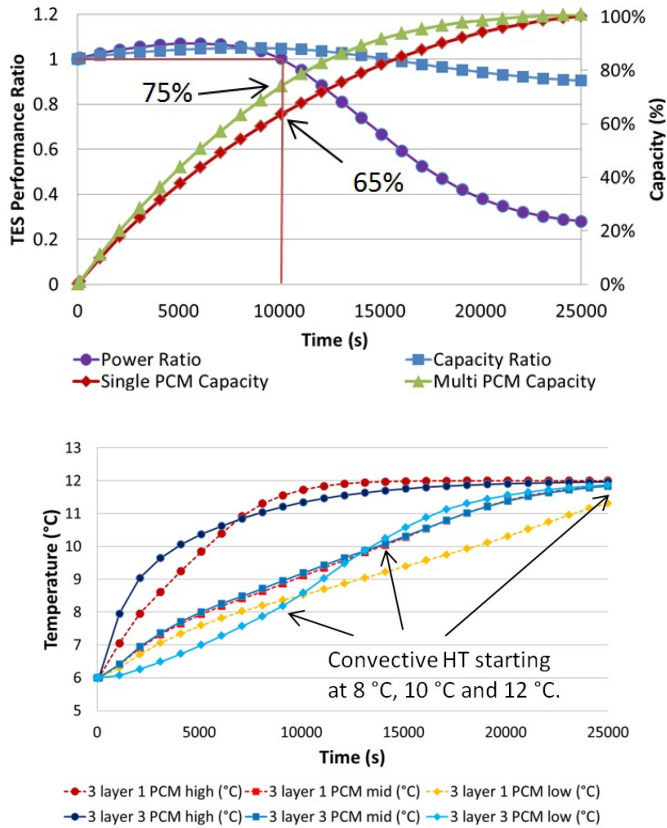


Figure 4-16 Performance Ratio (top) and Temperature Profile in Discharge (bottom)

Here, as the multi-PCM storage drops in thermal power rate (power ratio of less than 1), the rate of increase in multi-PCM capacity slows down. The storage capacity of the single and the multi-PCM units converge together. In the melting process, the storage capacity reaches full capacity, while in the freezing process, only 85% of the full performance was reached due to slower freezing rate because of the increased thermal resistance as solid builds up.

Figure 4-17 presents the ratio of melting to freezing thermal power rate for single-PCM and multi-PCM based LHTESs. The melting thermal power rate is higher than the freezing thermal power rate up to 95% of the single-PCM storage full charge capacity, and up to 70% of the multi-PCM storage full charge capacity. It is seen here that the multi-PCM TES provides a more symmetric melting/freezing thermal power ratio varying within  $\pm 20\%$  up to 80% of the full capacity. While the single-PCM TES favors melting process than freezing with up to 50% difference.

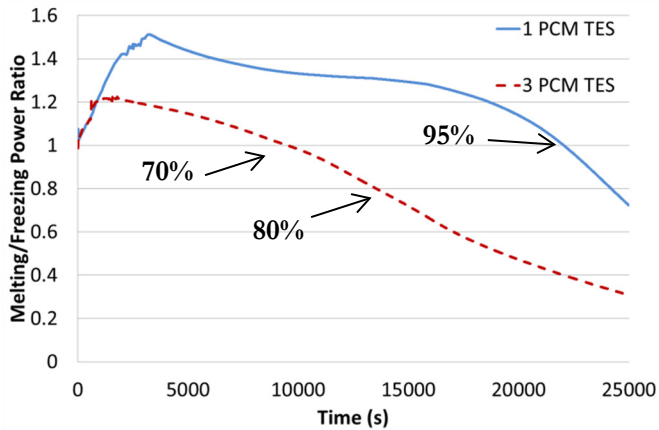


Figure 4-17 Melting and Freezing Thermal Power Comparison

In real applications, full storage cycling may not be possible, as it is resource and load dependent. A continuous half-charge/discharge cycling study was thus performed to examine the dynamics of a storage unit. The allotted charge/discharge time suffices to charge 30% and 25% of the full theoretical capacities of multi and single PCM, respectively. A series of 5 half charge/discharge cycles were considered, and the TES performance ratios are shown in Figure 4-18.

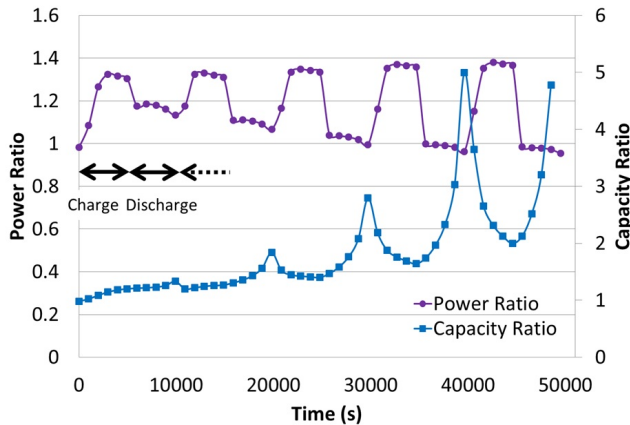


Figure 4-18 Storage System Dynamics in Charge and Discharge

The results show that the charging power ratio tends to increase through continuous cycling and converges towards a ratio of 1.4. The discharging power ratio, on the other hand, begins at 1.2, but then drops below 1 after five cycles. As a matter of fact, the single-PCM TES has higher discharging (melting) rate than charging (freezing) rate, hence small discharging power ratio which is the ratio of multi-PCM thermal

power to single-PCM thermal power. As the discharge power ratio is smaller than the charging power ratio, the capacity ratio is shown to soar continuously at the end of each of the continuous half charge/discharge cycles. To further clarify the possible reasons behind higher charge power ratio as compared to the discharge power ratio, the temperatures in the three layers of the TES are presented in Figure 4-19, for both multi-PCM and single PCM TESs.

PCM in both the multi and single-PCM configurations were initialized at 12 °C. Each of the three stages in multi-PCM TES reaches their respective phase change temperatures, at 7 °C, 9 °C, and 11 °C. The single-PCM (9 °C) also manifests the same; however, the top layer PCM temperature tends to fluctuate between the inlet heating temperature and its phase change temperature (9 °C) while the bottom layer PCM temperature reaches towards the inlet cooling temperature. As the bottom layer of the single-PCM TES diverges from its phase change temperature of 9 °C to a lower temperature level, the discharging (melting) power rate of the single-PCM TES improves due to a larger temperature driving force, charging (freezing) thermal rate is on the other hand lowered due to smaller temperature driving force. The drop in the temperature of the bottom layer but not in the top layer of the single-PCM TES is due to non-symmetry of  $c_p$ . Furthermore, an increase in capacity ratio after a number of cycles is observed, this is due to faster discharge of the single-PCM TES than the multi-PCM TES, hence a larger capacity ratio of the multi-PCM to the single-PCM TES.

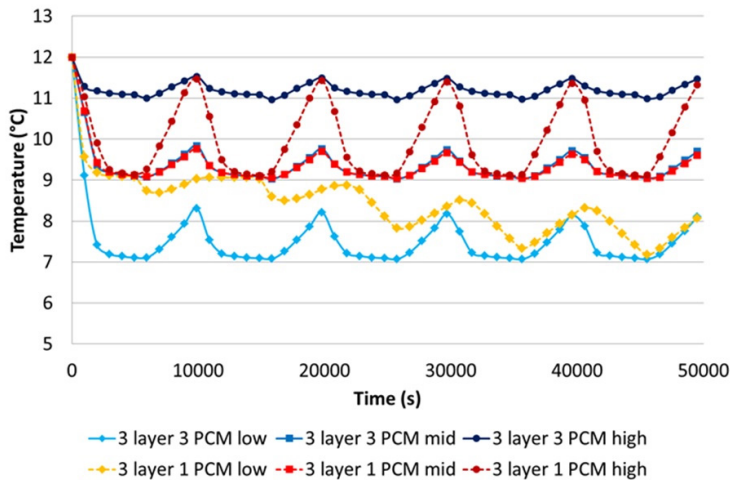


Figure 4-19 Temperature Profiles of PCMs at Different Layers

## 4.5 Concluding Remarks

In this section, numerical modeling was performed and validated with experimental study. The conduction only heat transfer model was shown to be within 5% time difference from the gelled PCM based LHTES. The non-gelled PCM based LHTES was modeled with conduction/convection heat transfer mechanisms and the results were within 15% time discrepancy. An additional study performed here showed that the fin spacing in submerged finned pipe heat exchanger configuration affects the contribution of natural convective heat transfer performance in non-gelled PCM based LHTES. It may be concluded that with fins spaced less than 15 mm apart, the natural convection is almost negligible for non-gelled PCMs. In the goal of reaching high enough thermal power rate, the concept of a multilayered multi-PCM based TES system was studied and was shown to reach 40% higher performance rating in the freezing process and 10% higher performance rating in the melting process than a single PCM TES unit. Continuous half charge/discharge cycling of multilayered multi-PCM storage demonstrates the tendency of the system reaching higher cold storage level due to more enhanced freezing rate. For applications where charge/discharge rates are of equal importance, multi-PCM based TESs also prove to be more suitable, as the melting and the freezing rates are more comparable. In the following section, the focus will be moved from component level design to system integration optimization.

# 5 Active Cooling Storage System Integration

This section is based on paper III and paper IV. Active TES that stores off-peak thermal energy for use during the on-peak period is the focus of this study. This type of TES system contributes towards positive energy building with storage of free night time cooling or off-peak renewable resource based energy for day time cooling purpose.

A techno-economic comparison of various types of TES integrated to an office building in Stockholm is first assessed. The viability of such a solution serves as a basis for the second study where TES optimization in a passively designed seminar room is performed.

## 5.1 TES in District Cooling Network

The load profile of an office building in Stockholm was considered in this study. The office building is connected to the Stockholm district cooling network and exhibits large day-to-night cooling demand variation. The aim here is to achieve peak thermal demand shaving. Stratified chilled water storage (SCW), auxiliary chiller (AC) and LHTES were compared against one another in terms of techno and economic viability.

The office building has a peak thermal load of 271 kW and an average load of 139 kW. TES in our scenario is used for dry cooling where 14 °C inlet temperature is required. In the charging mode, 8 °C feed water runs through the storage; in discharging mode, cold is pumped out from the unit to provide cooling at 14 °C, see Figure 5-1.

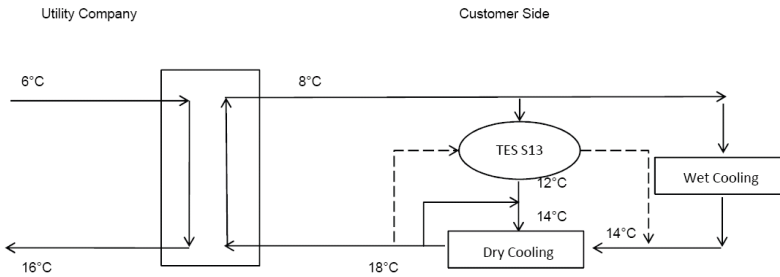


Figure 5-1 Schematics of TES Charging (continuous line) and Discharging (dashed line)

PCM with a phase change temperature of 13 °C is used. The chosen PCM is a commercialized salt-hydrate S13 (PCMProducts, 2009). In the charging mode, the HTF is heated from 8 °C to 12 °C while cooling down the TES. In the discharging mode, the HTF is cooled down from 18 °C to 14 °C to provide dry cooling to the building during peak-hours.

Key figures are shown in Table 5-1, more detailed input information is given in the corresponding paper IV appended to this thesis.

Table 5-1 Model Input

PCM	Salt Hydrate S13	Heat exchanger	Finned Pipe
Latent heat capacity	140 kJ/kg (208 MJ/m <sup>3</sup> )	Heat transfer coefficient	117 W/m <sup>2</sup> .K
Thermal conductivity	0.43 W/m.K	Storage tank cost	350 €/m <sup>3</sup> to 1460 €/m <sup>3</sup>
Subcooling	<1 °C	Space renting	80 €/m <sup>2</sup> .yr
PCM cost	130 €/kWh	Auxiliary chiller	400 €/kW
Electricity tariff	7 ¢/kWh		

An economic feasibility study was performed comparing LHTES against SCW and conventional AC. The results are aimed at identifying the cost effective LHTES installation, and are summarized in Table 5-2. In the Stockholm district cooling network, the customers are charged based on the cooling network flow rate and not on the actual extracted energy, this is denoted in the table as a *penalty*. The intention of the current *penalty* mechanism in Stockholm is to maintain the return tempera-

ture on the district cooling line above 16 °C (refer to Figure 5-1) as the customer always pays for the energy amounting to the value obtained for a certain flow rate multiplied by the assumed temperature change 6 °C supply/16 °C return. If the return temperature is lower, i.e. 14 °C, then the customer thus still pays for the energy as if it had been the desired return temperature of 16 °C.

A scenario where the PCM cost is reduced by 50% was also investigated. It is shown here that under *penalty* and without any cost reduction, the LHTES is economically viable against SCW if less than 5% of the peak power is to be shaved, and that the LHTES is economically viable against an electric driven chiller if 1% to 9% of the peak power is to be shaved. By taking away the *penalty* described above, and by assuming half the PCM cost, the LHTES is viable up to 30% peak shave against SCW and viable from 1% to 22% peak shave against chiller. As a general remark, in all cases where LHTES is not economical viable, SCW is more cost effective than the AC system.

Table 5-2 Cost Effective Peak Power Reduction Rate <sup>4</sup>

	SCW	Auxiliary Chiller
Penalty/ No Cost Reduction	<5%	1%-9%
Penalty/ 50% Cost Reduction	<7%	1%-14%
No Penalty/ No Cost Reduction	<9%	1%-11%
No Penalty/ 50% Cost Reduction	<30%	1%-22%

At cost breakeven point between the LHTES and the SCW, the cost breakdown in Figure 5-2 illustrates the cost intensive PCM in LHTES overall cost and the high cost share of the SCW storage tank due to the large storage size. It is seen here that PCM represents around half of the total LHTES cost and the tank in SCW configuration also represents around half of the total cost. From this study, we reached the conclusion that if a larger storage size is needed, the increase in PCM cost will surpass that of the SCW tank cost and thus render LHTES less economical.

<sup>4</sup> Based on a 5-day load profile

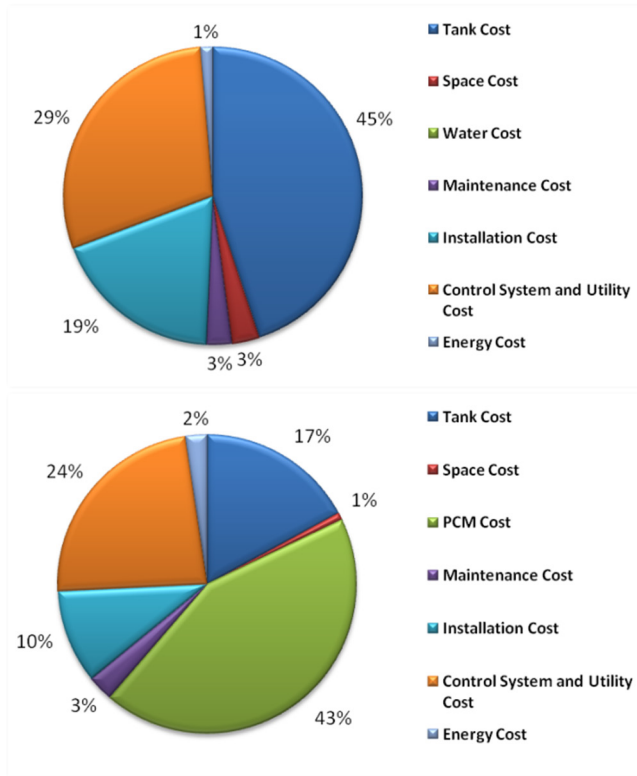


Figure 5-2 SCW (top) and LHTES (bottom) Cost Breakdown at Cost Break Even

We have shown that due to nonlinear cost variation of the LHTES, the SCW and the auxiliary chiller, LHTES is in general more cost-effective in providing small peak shave, SCW is better for medium amount of energy load management, while chillers are better for large load managements. This conclusion leads to the next study where optimization of LHTES in terms of heat exchanger design, equipment size, and energy use is performed.

## 5.2 LHTES System Optimization

Passive building has gained increasing attention as heating requirement is lowered during cold seasons, however in warmer seasons, the cooling demand is more intensive (Badescu et al., 2010) (Mlakar & Strancar, 2011). In this section, latent heat storage of night time cooling for day time use is optimized. A passive design based seminar room conform to Swedish regulation (BBR, 2011) is built in TRNSYS v16.1. Key modeling inputs are shown in Table 5-3.

Table 5-3 Model Input

Description	Value
Window to living space ratio	<20%
Heat transfer coefficient of building envelop	0.21 W/m <sup>2</sup> .K
Air exchange rate	8 l/s.occupant
Infiltration rate	0.07 vol/h (Persson M.L., 2006)
Internal lighting	15 W/m <sup>2</sup> (Li et al., 2010)
Occupants' metabolic rate	60 W/m <sup>2</sup> (Geneva, 1989)
Seminar room dimension (l*w*h)	9 m * 6 m * 3 m

A simulation of the passive structure under Stockholm climate condition in theoretically perfect conditions indicates overheating of the interior during day time in summer. Without any air exchange from and to the ambient environment, indoor temperature soars to 80 °C. This is however a theoretical “extreme” case where even infiltration is suppressed. While with ventilation complying to the building regulation, and by taking into account infiltration, the interior still reaches 40 °C, Figure 5-3. Peak cooling demand of around 3 kW during day time is shown to be needed to bring down the indoor temperature to a maximum of 26 °C, which is set to be the maximum allowable indoor temperature. It is presented from the previous study in section 5.1 that LHTES is one of the most promising solutions for small peak shaving. LHTES is thus considered for displacing this peak marginal cooling demand from night time free cooling to day time use.

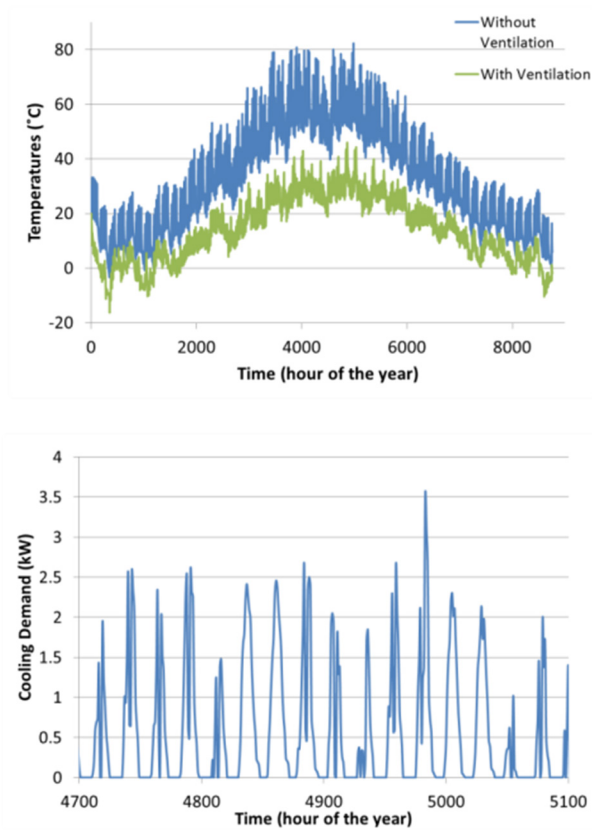


Figure 5-3 Indoor Temperature with and without Ventilation (top) and Cooling Demand (bottom)

LHTES is integrated to the ventilation system in this study. Three working modes are adapted in the system modeling. They are 1: charging of LHTES with outdoor cold air, 2: standby mode, 3: discharging of cooling to the interior, Figure 5-4.

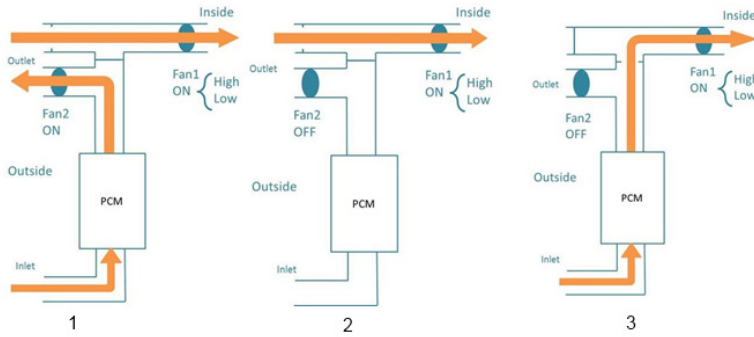


Figure 5-4 Working Modes (left to right 1: charging, 2: standby, 3: discharging)

The choice of PCM depends heavily on the resource availability, the working temperature range and the load profile. In Figure 5-5, for high cooling thermal power rate demand, a large driving temperature difference is required, so a PCM with low phase change temperature is more suitable; however the charging power of cold will be reduced and the regeneration time is hence increased. On the other hand if a PCM with higher phase change temperature is utilized, the charging of cold can be achieved at a higher thermal power rate, while the provision of cooling power will be hampered. For an equal charge/discharge thermal power rate in the warmest season of the year, a PCM with the average summer outdoor temperature as a phase change temperature is recommended (Arkar et al., 2007) and (Medved & Arkar, 2008). A commercial PCM with phase change temperature of 17 °C is hence taken to fit Stockholm climate condition.

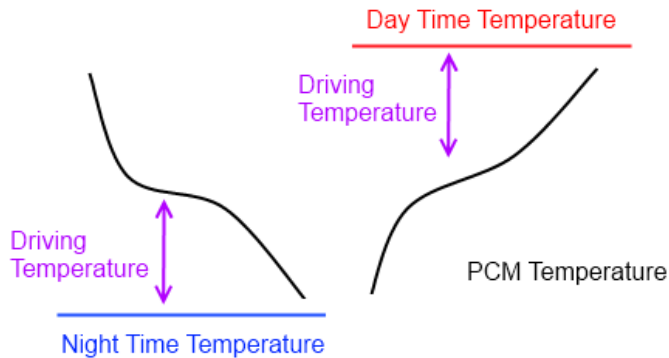


Figure 5-5 Charge and Discharge Potential

A system cost is calculated based on 4.5 €/kg PCM market price, 1.1 €/kg heat exchanger aluminum cost, 230 €/m<sup>2</sup>-yr space rental cost and Swedish electricity tariffing system, refer to Table 5-4. The auxiliary

chiller is taken at 385 €/kW specific installation cost. The life span of both storage and chiller is taken as 15 years.

*Table 5-4 Swedish Electricity Tariff from One Major Power Company in 2010*

#	Item	Description
1	Electricity Price	51.42 öre/kWh (average over July/Aug/Sept 2010)
2	Electricity Contract Fee	3.1 öre per hour
3	Energy Tax	28 öre /kWh
4	VAT (25%*(#1+#2+#3))	based on #1, #2 and #3
5	Grid Contract Fee	7.4 öre per hour
6	Grid Fee	23.92 öre /kWh
7	VAT (25%*(#5+#6))	based on #5 and #6

### 5.3 Sensitivity Analysis

An optimization of LHTES with objective functions set to match the highest cooling demand and the lowest system cost was conducted. Special acknowledgement is given to the Industrial Energy Systems Laboratory of the Swiss Federal Institute of Technology where the multi-objective optimization algorithm was developed. Acknowledgement also goes to the University of Graz for providing the LHTES component 842 in TRNSYS v16.1. The studied parameters are heat exchanger design, HTF pump size and PCM capacity. The Pareto Optimal front of the optimal LHTES design is shown in Figure 5-6 where x axis represents the normalized system cost defined as the ratio of the total TES system cost to the AC cost and y axis shows the remaining cooling demands. Each of the dots shown in the graph represents a different configuration of LHTES. For instance, at around 30% of the normalized system cost, one configuration will lead to 60% of remaining cooling need, while the optimal configuration corresponds to 32% of the remaining cooling need. The auxiliary chiller is also marked in the graph where full cooling demand is met at 100% normalized system cost.

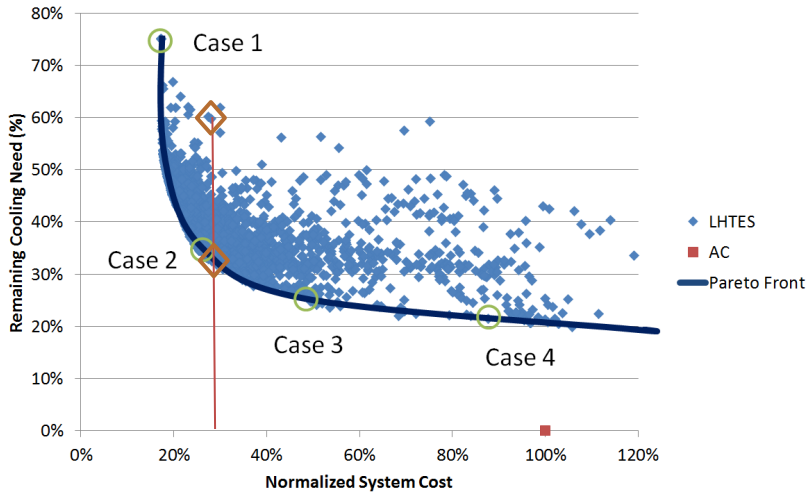


Figure 5-6 Pareto Optimal Front

The Pareto Optimal front is the curve linking all the most optimized configurations that a LHTES can have to reach the lowest cost and the smallest remaining cooling demand. The general trend shows an 80/20 rule where at 20% lower cost, the LHTES may supply slightly below 80% of the cooling demand; and at 80% lower cost, LHTES fulfills slightly above 20% of the cooling demand. It is shown here that approximately 1/5 of the total cooling demand cannot be met with night time cooling based LHTES at cost break with electrically driven AC in this specific scenario; certain comfort or economic tradeoff has thus to be considered for the use of free night time cooling.

Four specific optimal configurations are chosen for further analysis, they are presented here in Figure 5-7, the cases correspond to low cost/high remaining cooling need, high cost/ low remaining cooling need and two intermediate cases (as indicated in Figure 5-6). The lowest cost configuration utilizes the least amount of electricity, but leaves a large amount of the cooling demand unmet. The lowest remaining cooling demand scenario has the most cost-efficient heat exchanger configuration, but the high HTF pumping power demand contributes to an increase of the overall electricity use. Case 2 and case 3 have the same electricity consumption but with varying cost to remaining cooling demand due to different heat exchanger component designs.

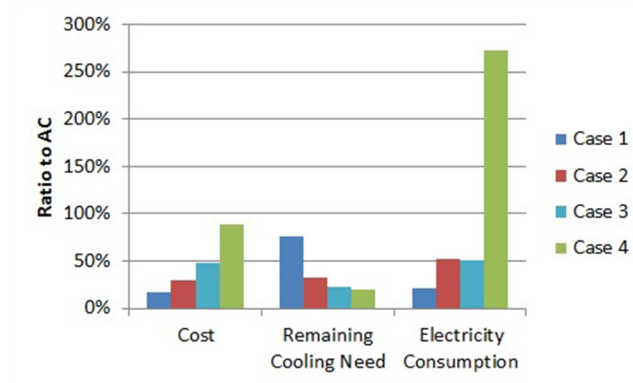


Figure 5-7 Comparison of Four Optimized LHTEs

It is remarked here that the electricity price inflation and the PCM cost fluctuation are omitted in the net present value calculation over the timespan of LHTEs in this study. This leads to a further study on the sensitivity of PCM cost and energy price on the overall LHTEs cost, as shown in Figure 5-8.

Case 1 and case 4 show the smallest dependency on PCM cost, while case 1 and the AC case show the highest dependency towards electricity price fluctuation as the share of electricity cost is high in both cases. Case 3 on the other hand exhibits the smallest fluctuation as regards to the increase in electricity tariff: 22% increase for 50% higher electricity cost, whereas the AC presents over 40% cost increase. This sensitivity analysis indicates the high potential of LHTEs cost reduction in the upcoming years where lower PCM cost and increasing electricity tariff are very likely to occur in the business as usual scenario.

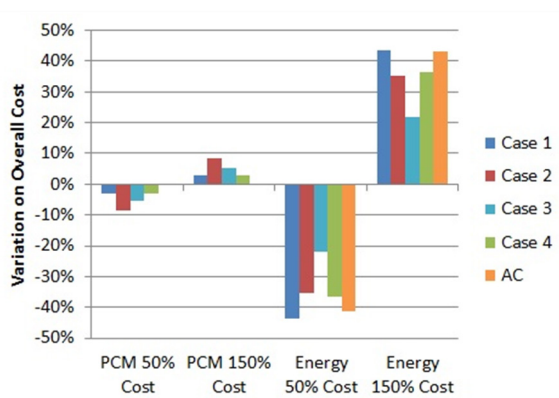


Figure 5-8 Sensitivity Analysis of System Cost to PCM Price and Energy Tariff

Coefficient of performance (COP) indicates the level of energy efficiency a system has. The COP is calculated based on the following equation:

$$\text{COP} = \frac{\text{Thermal Output}}{\text{Electricity Input}} \quad \text{Eq. 5-1}$$

The COP of the AC is taken as 3 in this study. The COPs obtained for cases 1 to case 4 are presented in Table 5-5. It is seen here that case 1, 2 and 3 have higher COP as compared to the AC system, while case 4 only has a COP of around 1. From the energy efficiency perspective, higher COP leads to higher energy saving, however the saving is not always reflected in the overall system cost.

Table 5-5 Coefficient of Performance

	COP
Case 1	3.97
Case 2	4.57
Case 3	5.30
Case 4	1.03

## 5.4 Concluding Remarks

LHTES can be successfully used for peak shaving in both district cooling network to expend cooling capacity and in independent buildings to increase the use of renewable resources. It is shown from the first study that smaller LHTESs are more economically viable as storage tank cost is not linear to the storage size. In the second study, we conclude that tradeoff between comfort level and use of renewable energy is inevitable if economic ground is to be reached. Nonetheless, with ever increasing energy price and with maturing PCM technology, LHTES may well in the near future be techno-economically viable while complying with comfort level in the context of reaching sustainable development goals.

The final research question raised is the quantification of environmental benefit with use of TES for thermal peak shave and load shift. The outcome will be presented in section 6, where integration of TES in the Swedish society is studied and environmental benefit accounted for.



# 6 Environmental Benefits of TES

Anthropogenic use of fossil fuels is the main cause to global GHG emissions. It has been asserted that 30% of fauna and flora will face extinction in the 21<sup>st</sup> century (IPCC, 2007). In the goal of limiting global warming, several scenarios have been proposed, e.g. the BLUE scenario bringing emissions to half of 2005 level by 2050, or the ACT scenario bringing emissions to 2005 level by 2050 (IEA, 2008). To reach any of these goals, reduction of fossil fuel based energy use is to be achieved. The majority of cost effective renewable energy sources, e.g. large scale hydropower and high temperature geothermal, have been exploited (EIA, 2011). Other renewable energy sources, such as solar and wind, present however drawback with intermittent resource availability. Energy storage systems have shown potentials in maintaining constant power generation, in leveling user load demand, and in utilizing waste heat/free cooling (Anisur et al., 2013). In this chapter, the potential of mitigating GHG emissions in the Swedish residential and service sector will be explored. This section is based on paper VII.

## 6.1 Overview of Swedish Energy Use

Over 45% of the total residential and service sector energy use in Sweden goes to indoor heating and cooling (Swedish Energy Agency, 2009). The distribution of indoor thermal comfort energy use varies from summer to winter due to climatic factor. The increase of heating demand can be partly seen through the increase of Swedish monthly marginal electricity production and import in Figure 6-1. The increase of conventional thermal power generation indicates double to triple of the off-peak season, i.e. 700 GWh of electricity was produced in July 2009 against 2500 GWh in Feb 2010. Wind power is shown here to depict the resource dependency of renewable energy where modulation in production is impossible.

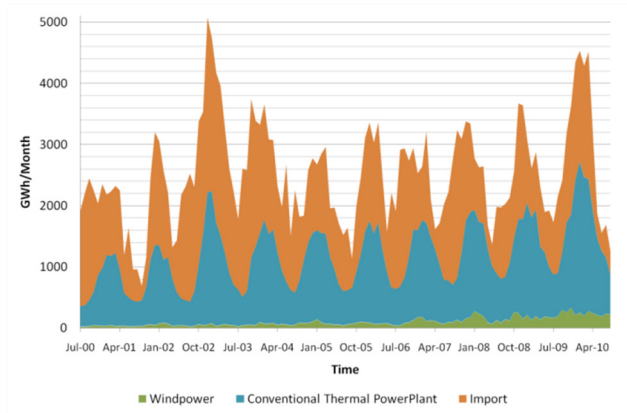


Figure 6-1 Swedish Peak Electricity Flow (from wind, thermal power and import) in Sweden 2000-2010, adapted from (ENTSOE, 2011)

In 2010, 146 TWh of electricity was generated in Sweden with fossil fuel based conventional power production means contributing to 4.3 TWh (ENTSOE, 2011). District heating network provided 68 TWh where 17.5% is still fossil fuel based (Swedish Energy Agency, 2011). Furthermore, 7% of the total Swedish residential and service sectors are still equipped with individual oil burner and 23% with electric heating systems, Figure 6-2 (left). The distribution of total fossil fuel use in heating of the residential and service sectors is mainly attributed to peak district heating production (59%) and individual oil burners use (37%), Figure 6-2 (right). The goal of this section is to determine the potential of using energy storage to peak shave marginal fossil fuel based energy supply.

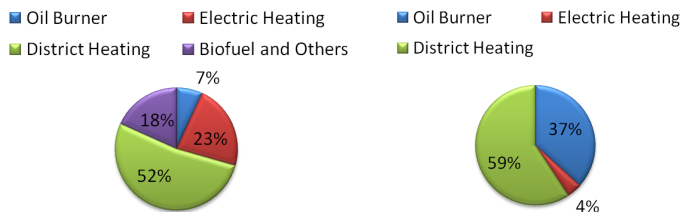


Figure 6-2 Heating Means (left) and Fossil Fuel Use (right) in Heating of Residential and Service Sectors

## 6.2 Methodology and Model

The methodology consists of replacing marginal fossil fuel based peak energy demand with TES systems that store off-peak nonpolluting energy for use during peak hours. The storage is placed between the utility company and the user, benefitting thus both parties. The payback of TES installation is achieved with cost saving from avoided fossil fuel

use. The CO<sub>2</sub> emission level by fossil fuel type is shown in Table 6-1, and the Swedish emission tax is presented in Table 6-2.

Table 6-1 CO<sub>2</sub> Emission by Fuel, adapted from (IEA, 2010), (Arve et al., 2011)

	Specific Carbon Content (kg C/kg fuel)	Specific Energy Content (kWh/kg fuel)	Specific CO <sub>2</sub> Emission (kg CO <sub>2</sub> /kWh)
Coal	0.75	7.5	0.37
Gas	0.75	12	0.23
Fuel Oil	0.7	11.7	0.26

Table 6-2 Emission Tax in Sweden (currency converted to US\$) (Swedish Tax Office, 2010)

	CO <sub>2</sub> Tax	Total GHG Tax	Total Tax
Coal	350(\$/ton)	394(\$/ton)	5.5 (¢/kWh)
Gas	301(\$/1000m <sup>3</sup> )	335(\$/m <sup>3</sup> )	3.0 (¢/kWh)
Fuel Oil	402(\$/m <sup>3</sup> )	631(\$/m <sup>3</sup> )	5.4 (¢/kWh)

The cost of TES storage unit is modeled to follow a “learning curve”, further detail on the methodology is given by (Feroli et al., 2009), Eq. 6-1.

$$C = C_0 \left( \frac{X}{X_0} \right)^{-LP} \quad \text{Eq. 6-1}$$

where  $C_0$  is the initial unit cost,  $C$  is the current unit cost,  $X_0$  is the initial cumulative capacity,  $X$  is the current cumulative capacity and  $LP$  is the learning parameter.  $LP$  is a function of the learning rate (LR) expressed in Eq. 6-2.

$$LR = 1 - 2^{-LP} \quad \text{Eq. 6-2}$$

Feroli performed a review on LR of 108 applications and observed LR of industrial product in the range of 3% to 34% (Feroli et al., 2009). The initial LR of TES in this study is taken the same as that of a thermal comfort air conditioning: 10%, then a gradual slowdown to 5% is introduced at 10 MWh cumulated TES capacity.

The linear optimization is performed to give the minimum peak shaving cost (PSC), this function is expressed as the difference of TES cost (TESC) to the generation cost reduction (GCR) and to the avoided fossil fuel cost (AFFC), Eq. 6-3.

$$\text{PSC} = \text{TESC} - \text{GCR} - \text{AFFC} \quad \text{Eq. 6-3}$$

GCR is the sum of the fixed operation and maintenance (FOM) cost and the variable operation and maintenance (VOM) cost weighted with the peak shaved power (PSP) and peak shaving load capacity (PSL) respectively, Eq. 6-4. Here the discount rate (R) is taken at 6% and the life expectancy (N) is taken as 20 years.

$$\text{PCR} = \text{PSP} * \left\{ \text{FOM} * \frac{1 - (1 + R)^{-N}}{R} \right\} + \text{PSL} * \left\{ \text{VOM} * \frac{1 - (1 + R)^{-N}}{R} \right\} \quad \text{Eq. 6-4}$$

The avoided fossil fuel cost is the sum of fuel cost (C) weighted to the fuel reduction share (FRS), Eq. 6-5.

$$\text{AFFC} = \text{FRS}_{\text{Coal}} * C_{\text{Coal}} + \text{FRS}_{\text{Gas}} * C_{\text{Gas}} + \text{FRS}_{\text{Oil}} * C_{\text{Oil}} \quad \text{Eq. 6-5}$$

### 6.3 Results and Discussion on CO<sub>2</sub> Mitigation Potential

Modeling results show that 620 kTon of annual CO<sub>2</sub> emissions can be reduced cost effectively through peak shave with use of TES in the Swedish heating sector. Figure 6-3 shows the distribution of CO<sub>2</sub> reduction by means of heating. The oil burner is shown to have the largest CO<sub>2</sub> mitigating potential representing 80% of total achievable CO<sub>2</sub> emission reduction. The required TES installation amounts to 14 GWh storage capacity replacing 2.5 TWh of fossil fuel based energy generation.

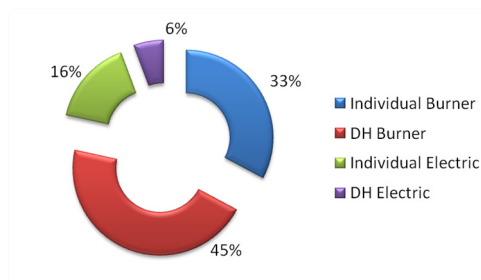


Figure 6-3 CO<sub>2</sub> Emission Reduction by Means of Heating

Here, the study is performed on replacement of marginal fossil fuel produced energy with TES for indoor heating in the Swedish residential and service sector. The incentives behind the cost effectiveness are mainly CO<sub>2</sub> tax reduction and fossil fuel cost avoidance. It is however to be noted that the off-peak renewable energy produced thermal energy was considered as free extra capacity in our model. Future work is to be conducted to determine the technically feasible peak fossil fuel reduction.



# 7 Concluding Discussions

Thermal energy storage is one of the technologies that may contribute to energy conservation through peak energy load alleviation, energy demand shift, and free cooling/waste heat utilization. In the thermal comfort temperature range, heat storage can be achieved with a stratified hot water storage unit. However, cold storage requires a larger storage volume if sensible thermal energy storage is utilized (such as stratified chilled water) due to smaller allowable working temperature range. LHTES has an advantage in storing a high amount of thermal energy with small temperature swing through use of phase change materials (PCMs) as storage mediums. One of the most common PCMs is ice/water, however the low phase change temperature of ice/water makes them a less desirable PCM for indoor comfort cooling. A relatively large number of other phase change materials with different phase change temperatures have been tested and studied in recent years. The work presented herein has contributed to the knowledge of LHTES as follows:

- Assessment and validation of the novel material characterizing T-history method
- Development and theorization of numerical models for design of storage component
- Optimization of system integration and evaluation for climate change mitigation solution

## 7.1 Concluding Remarks

PCMs are divided into organics and inorganics; the former have better compatibility with metallic storage containers, small subcooling issues, and no phase segregation, while the latter shows higher volumetric storage density and non-flammable advantage for use in buildings. The caveats with PCMs in general are their low thermal conductivity which limits the thermal power rate for charge and discharge in active TES systems where high load demand is needed; relatively high material cost is yet another limiting factor for wider spread of the technology; finally, lack of reproducible PCM thermal property data is the cause for system design uncertainties.

The T-History method is a relatively novel material property testing procedure for characterizing enthalpy change of an unknown material by comparing with a known reference sample. The accuracy of the method is however highly dependent on good sensitivity of the temperature sensors, on reproducible heat flux to both the reference and the tested samples, on low Biot number, and on good knowledge of the reference material. This thesis further contributes to an advanced calculation scheme for determination of material's thermo physical property and analysis of T-History setup orientation where the horizontally placed sample holder is favored over the vertically placed sample holder for buoyancy restriction.

A simplified adapted Dirac delta function is shown to adequately represent the specific heat capacity of PCMs within certain limitations with need of only two function parameters. It fits experimental data well, and is here shown to represent the specific heat capacity in modeling by enabling the characteristics of a phase change to be adequately captured.

A finite-difference enthalpy-based conduction model was verified to be within 5% time difference against experimentally obtained data for gelled salt-hydrate PCM based LHTES in terms of charge/discharge performance assessment. From this work, it is observed that the melting process took 13% longer time than the freezing process. Preliminary explanations are the non-symmetric PCM enthalpy profiles, the hysteresis in melting and freezing enthalpy and the larger phase change temperature range in melting as compared to freezing.

A conduction/convection model was further developed for assessment of non-gelled storage performance. Convection is controlled with change of material viscosity above and below the phase change temperature; experimental and numerical results are within 15% time difference. The larger discrepancy between numerical model and the experimental reading is mainly due to uncertain regarding the cutoff point of convective heat transfer mechanism in the mushy region where PCM is in both liquid and solid states.

In the goal of improving the heat transfer rate of an active LHTES unit, the effect of convective heat transfer and fin spacing was studied. It is shown that densely packed submerged finned pipe heat exchanger provides higher thermal power rate due to the larger heat exchange surface area. On the other hand, such a heat exchanger configuration brings down the PCM packing factor, resulting in a smaller volumetric storage capacity. Depending on the resource availability for cycling of LHTES and on the thermal energy power rate demand, an optimization of the LHTES design is required for reaching high enough recycling thermal

power rate and high storage capacity while maintaining cost effectiveness.

To further improve the LHTES thermal power rate, a multi-PCM filled storage unit was proposed. The concept consists of maintaining the HTF to PCM temperature difference to reach higher charge/discharge rate. Simulation of a multi-PCM LHTES demonstrates peak freezing performance improvement of 40% and peak melting performance improvement of 20%. In real applications, full charge and full discharge may not be fully attained at each cycle. Here, five continuous half charge and half discharge cycles were performed; the results indicate similar freezing performance enhancement but a decrease in melting performance enhancement from 20% to none. In absolute terms, the melting rate is higher than the freezing rate in single-PCM based LHTES. The multi-PCM concept enhances the freezing rate and brings down the gap between charge and discharge thermal power rate. Here, both the non-symmetry of PCM enthalpy profile and the convective heat transfer mechanism that is less present in freezing contribute to the higher freezing rate enhancement with multi-PCM concept. The understanding of this storage component dynamic is essential in achieving well-functioning LHTES design.

Having the storage component model evaluated, integration of LHTES to an energy system was then investigated. Through techno-economic comparison of the LHTES, the SCW storage and the AC systems, techno-economic integration of energy storage to district cooling network connected office building in Stockholm was assessed. It is shown that LHTES reveals to be cost effective for low peak shave (< 5%) with Stockholm's current district cooling tariff scheme where the fee is charged by the flow rate. By comparing LHTES to an AC system, the LHTES is cost effective up to a higher level of peak shave (< 9%). It is crucial to point out that without this *penalty* caused by the flow rate based tariff scheme, and for a 50% cost reduction for PCM, LHTES may be cost effective for shaving up to 30% of peak load as compared to SCW, and up to 22% as compared to AC. For cases where space is limited on a district cooling connected network, LHTES is an alternate solution besides SCW and AC for providing additional thermal load demand and for reducing peak power use. In all cases, TES is more cost effective than AC system for peak load shaving of a district cooling network connected office building.

To cut down the winter heating demand, passive buildings are fitted with high thermal insulation layers, this causes however overheating in the summer time due to excessive internal heat gain in public buildings such as schools, office buildings, shopping centers and hospitals. In-

creased day time cooling demand has thus been identified. In Sweden where night time air temperature drops to a level suitable for indoor cooling, integration of LHTES to a passive seminar room for free night-cooling load displacement was evaluated and LHTES configuration optimization was performed in this thesis. It is shown that with certain tradeoff to comfort level, LHTES using night time cold for day time cooling proves to be a cost competitive solution as compared to electrically driven auxiliary chiller. Furthermore, the study shows that with different LHTES configurations, the same capital intensive storage system may be reached with various levels of electricity consumption, different amounts of PCM, diverse sizes of ventilation unit and heat exchanger design options. The optimally designed LHTES should use the least amount of electricity for air venting while providing the highest amount of thermal displacement. In this specific case study, 75% of the total cooling demand at half of the conventional AC cost can be reached.

Finally, the question on environmental adequateness is raised: can TES reduce GHG emissions? An investigation on the potential of peak shaving was performed and the result shows positive outcome, peak shaving through thermal energy load shift does reduce marginal fossil fuel based energy consumption. The largest share of fossil fuel use that can be displaced is in district heating where marginal oil burners are still used. Individual oil burners that are commonly used in remote houses are however less susceptible to be replaced with TES as fewer other heat producing options are available. As a result, a conservative estimation shows that about 2 TWh of district heating based fossil fuel burner can be cost effectively substituted with non-marginal heat production means through load shift, and 0.5 TWh of nationwide peak fossil fuel based electricity generation means can be alleviated through peak shave. This corresponds to 620 kTon of GHG emission or 13% of the total fossil fuel based emissions reduction from the Swedish residential and service sectors. It is noted here that this CO<sub>2</sub> reduction figure contributed from TES is in addition to the existing storage systems and mechanisms that are in place in the Swedish energy system.

## 7.2 Future Work

Numerical simulation with the enthalpy method has here been established as an adequate tool for designing of LHTES. However, subcooling and non-symmetry of phase change temperature range are yet a property that has to be accounted for in the model to further improve accuracy of performance assessment. It is important to capture every degree of temperature change in the phase change process since temperature margins in comfort cooling application is very small, and it needs to be assured that e.g. freezing actually occurs. To have a charging

temperature slightly below the ideal freezing point may not be sufficient to ensure a phase change if sub-cooling is present.

In component heat transfer modeling, the natural convective heat transfer mechanism is controlled with material viscosity. The author suspects that the modeling result is highly affected by the choice of viscosity level in the mushy region where both solid and liquid phases are present. Further study may be carried out to characterize viscosity change of PCM in region where both liquid and solid phases coexist so as to give an improved accuracy of the component heat transfer model for LHTES.

Under the same operating conditions, a multi-PCM storage configuration enhances the heat transfer. This enhancement is larger for the freezing process than for the melting process. Further research in optimizing multi-PCM layout configuration shall be addressed in case specific studies, especially in continuous half charge/discharge storage cycling process.

Equating Earth's existence to 24-hour time, humankind has flourished over the past few milliseconds through discovery of energy resources. With novel technologies and work proposed in this thesis, combined with our willingness for social and behavioral change, the author believes that through energy conservation, we may most probably prolong humankind's prosperity for a few extra seconds.



## 8 Bibliography

Abhat, A., 1983. Low temperature latent heat thermal energy storage: heat storage materials. *Solar Energy*, p. 313–332.

Agyenim, F. & Hewitt, N., 2010. The development of a finned phase change material (PCM) storage system to take advantage of off-peak electricity tariff for improvement in cost of heat pump operation. *Energy and Buildings*, pp. 1552-1560.

Agyenim, F., Hewitt, N., Eames, P. & Smyth, M., 2010. A review of materials, heat transfer and phase change problem formulation for latent heat thermal energy storage systems (LHTESS). *Renewable and Sustainable Energy Reviews*, pp. 615-628.

Al-Abidi, A. et al., 2012. Review of thermal energy storage for air conditioning systems. *Renewable and Sustainable Energy Reviews*, pp. 5802-5819.

Al-Dabbas, M. & Al-Rousan, A., 2013. Energy extracted from underground rock area by using a horizontal closed loop system in Mutah University/Jordan. *Energy Conversion and Management*, pp. 744-750.

Almajali, M., Lafdi, K. & Prodhomme, P., 2013. Effect of copper coating on infiltrated PCM/foam. *Energy Conversion and Management*, pp. 336-342.

Anisur, M. et al., 2013. Curbing global warming with phase change materials for energy storage. *Renewable and Sustainable Energy Reviews*, pp. 23-30.

Arce, P. et al., 2011. Overview of thermal energy storage (TES) potential energy savings and climate change mitigation in Spain and Europe. *Applied Energy*, pp. 2764-2774.

Arkar, C., Vidrih, B. & Medved, S., 2007. Efficiency of free cooling using latent heat storage integrated into the ventilation system of a low energy building.. *International Journal of Refrigeration*, pp. 134-143.

Badescu, V., Laaser, N. & Crutescu, R., 2010. Warm season cooling requirements for passive buildings in Southeastern Europe (Romania).. *Energy*, pp. 3284-3300.

Bales, C., 2005. *TASK 32. Chemical and sorption storage Selection of concepts*, s.l.: Solar Heating and Cooling.

BBR, B., 2011. *Regelsamling för Byggande*. s.l.:Boverket.

Bird, R., Stewart, W. & Lightfoot, E., 2002. *Transport Phenomena*. 2nd ed. s.l.:Wiley.

BP, 2012. *BP Statistical Review of World Energy*, s.l.: BP.

Cabeza, L. et al., 2011. Materials used as PCM in thermal energy storage in buildings: A review. *Renewable and Sustainable Energy Reviews*, pp. 1675-1695.

Cabeza, L., Svensson, G., Hiebler, S. & Mehling, H., 2003. Thermal performance of sodium acetate trihydrate thickened with different materials as phase change energy storage material. *Appl. Therm. Eng.*, p. 1697–1704.

Castell, A. et al., 2008. Natural convection heat transfer coefficients in phase change material (PCM) modules with external vertical fins. *Appl. Therm. Eng.*, pp. 1676-1686.

Climator, 2012. *ClimSel*. [Online]  
Available at: <http://www.climator.com/en/climsel/>  
[Accessed 2013].

Costa, M., Buddhi, D. & Oliva, A., 1998. Numerical simulation of a latent heat thermal energy storage system with enhanced heat conduction. *Energy Conversion and Management*, pp. 319-330.

Dincer, I., 2002. On thermal energy storage systems and applications in buildings.. *Energy and Buildings*, Volume 34, pp. 377-388.

Dincer, I. & Rosen, M., 2011. *Thermal Energy Storage, Systems and Applications*. 2nd Edition ed. s.l.:Wiley.

EIA, 2011. *International Energy Outlook 2011*, s.l.: s.n.

ENTSOE, 2011. *Statistic Database.*, s.l.: s.n.

ENTSO-E, 2012. *European Network of Transmission System Operators for Electricity*. [Online]  
 Available at: <https://www.entsoe.eu/resources/data-portal/production/>  
 [Accessed 2012].

Farid, M., Khudhair, A., Razack, S. & Al-Hallaj, S., 2004. A review on phase change energy storage: materials and Applications.. *Energy Convers. Mgmt.*, pp. 1597-1615.

Feroli, F., Schoots, K. & Zwaan, B. C. C. v. d., 2009. Use and limitations of learning curves for energy technology policy: A component-learning hypothesis.. Issue 37.

Frusteri, F., Leonardi, V., Vasta, S. & Restuccia, G., 2005. Thermal conductivity measurement of a PCM based storage system containing carbon fibers. *Applied Thermal Engineering*, pp. 1623-1633.

Fukai, J., Hamada, Y., Morozumi, Y. & Miyatake, O., 2002. Effect of carbon-fiber brushes on conductive heat transfer in phase change materials. *International Journal of Heat and Mass Transfer*, pp. 4781-4792.

Furzeland, R., 1980. A comparative study of numerical methods for moving boundary problems. *J Inst Maths Applics*, p. 411–429.

G.-Roisman, T., Shapiro, M. & Shavit, A., 2011. Effect of double-diffusive heat transfer on thermal conductivity of porous sintered ceramics: Macrotransport analysis. *International Journal of Heat and Mass Transfer*, pp. 4844-4855.

Geneva, I. 8., 1989. *Ergonomics of Thermal Environments – Determination of Metabolic Heat Production*, s.l.: s.n.

Gong, Z. & Mujumdar, A., 1996. Cyclic heat transfer in a novel storage unit of multiple phase change materials. *Appl Therm Eng*, p. 807–815.

Grozdek, M., 2009. *Shifting and Storage of Cooling Energy through Ice Bank or Ice Slurry Systems - modelling and experimental analysis*.. PhD Thesis, Royal Insitute of Technology ed. Stockholm, Sweden: s.n.

Günther, E., Hiebler, S. & Mehling, H., 2006. *Determination of the heat storage capacity of PCM and PCM-objects as a function of temperature*.. New Jersey, s.n.

- Hasnain, S., 2000. Need for thermal-storage air-conditioning in Saudi Arabia.. *Applied Energy*, Volume 65, pp. 153-164.
- Hasnain, S. M., 1998. Review on sustainable thermal energy storage technologies, Part II: cool thermal storage.. *Energy Convers. Manage.*, Volume 39, pp. 1139-1153.
- Hauer, A. et al., 2005. *Advanced Thermal Energy Storage through Application of Phase Change Materials and Chemical Reactions – Feasibility Studies and Demonstration Projects*, s.l.: Advanced Thermal Energy Storage through Application of Phase Change Materials and Chemical Reactions – Feasibility Studies and Demonstration Projects.
- Herrick, C. S., 1982. Melt-freeze-cycle life-testing of Glauber's salt in a rolling cylinder heat store. *Sol. Energy*, pp. 99-104.
- Hinze, M. & Ziegenbalg, S., 2007. Optimal control of the free boundary in a two-phase Stefan problem. *Journal of Computational Physics*, pp. 657-684.
- Holman, J., 2002 . *Heat transfer*. s.l.:McGraw-Hill.
- Hong, H., Kim, S. & Kim, Y.-S., 2004. Accuracy improvement of T-history method for measuring heat of fusion of various materials.. pp. 360-366.
- Hosseinzadeh, S., Tan, F. & Moosania, S., 2011. Experimental and numerical studies on performance of PCM-based heat sink with different configurations of internal fins. *Applied Thermal Engineering*, pp. 3827-3838.
- IEA, 2008. *Energy Technology Perspectives*, s.l.: s.n.
- IEA, 2010. *CO2 emissions from fuel combustion*, s.l.: s.n.
- IEA, 2012. *Key World Energy Statistics*, s.l.: s.n.
- IEA, 2012. *World Energy Outlook*, s.l.: s.n.
- Incropera, F., DeWitt, D., Bergman, T. & Lavine, A., 2007. *Fundamentals of Heat and Mass Transfer*. Sixth ed. s.l.:Wiley.
- IPCC, 2007. *Fourth Assessment Report (AR4)*, s.l.: IEA.

Ismail, K., Alves, C. & Modesto, M., 2001. Numerical and experimental study on the solidification of PCM around a vertical axially finned isothermal cylinder. *Appl. Therm. Eng.*, pp. 53-77.

Javierre, E., Vuik, C., Vermolen, F. & Zwaag, S. v., 2006. A comparison of numerical models for one-dimensional Stefan problems. *Journal of Computational and Applied Mathematics*, pp. 445-459.

Kuznik, F., David, D., Johannes, K. & Roux, J.-J., 2011. A review on phase change materials integrated in building walls. *Renewable and Sustainable Energy Reviews*, p. 379–391.

Lane, G. A., 1992. Phase change materials for energy storage nucleation to prevent supercooling. *Sol. Energy Mater. Sol. Cells*, , pp. 135-160.

Lázaro, A. et al., 2006. Verification of a T-history installation to measure enthalpy versus temperature curves of phase change materials.. Issue 2168-2174.

Li, D., Cheung, K., Wong, S. & Lam, T., 2010. An analysis of energy-efficient light fittings and lighting controls.. *Applied Energy*, pp. 558-567.

Li, G., Hwang, Y. & Radermacher, R., 2012. Review of cold storage materials for air conditioning application. *International Journal of Refrigeration*, pp. 2053-2077.

London Canal Museum, 2013. *Ice Import*. [Online] Available at: <http://www.canalmuseum.org.uk/ice/iceimport.htm> [Accessed 2013].

Marin, J., Zalba, B., Cabeza, L. & Mehling, H., 2003. Determination of enthalpy temperature curves of phase change materials with the temperature-history method: improvement to temperature dependent properties.. Issue 184-189.

Martin, V., He, B. & Setterwall, F., 2010. Direct contact PCM–water cold storage. *Applied Energy*, pp. 2652-2659.

Medrano, M. et al., 2010. State of the art on high-temperature thermal energy storage for power generation. Part 2—Case studies. *Renewable and Sustainable Energy Reviews*, pp. 56-72.

Medrano, M. et al., 2009. Experimental evaluation of commercial heat exchangers for use as PCM thermal storage systems. *Applied Energy*, pp. 2047-2055.

- Medved, S. & Arkar, C., 2008. Correlation between the local climate and the free-cooling potential of latent heat storage.. *Energy and buildings*, pp. 429-437.
- Mehling, H. & Cabeza, L. F., 2008. *Heat and cold storage with PCM*. s.l.:Springer.
- Mehling, H., Hiebler, S. & Günther, E., 2010. New method to evaluate the heat storage density in latent heat storage for arbitrary temperature ranges. *Applied Thermal Engineering*, pp. 2652-2657.
- Mesalhy, O., Lafdi, K. & Elgafy, A., 2006. Carbon foam matrices saturated with PCM for thermal protection purposes. *Carbon*, pp. 2080-2088.
- Mills, A., Farid, M., Selman, J. & Al-Hallaj, S., 2006. Thermal conductivity enhancement of phase change materials using a graphite matrix. *Applied Thermal Engineering*, pp. 1652-1661.
- Mlakar, J. & Strancar, J., 2011. Overheating in residential passive house: Solution strategies revealed and confirmed through data analysis and simulations.. *Energy and Buildings*, pp. 1443-1451.
- Nakaso, K. et al., 2008. Extension of heat transfer area using carbon fiber cloths in latent heat thermal energy storage tanks. *Chemical Engineering and Processing*, p. 879–885.
- Oró, E. et al., 2012. Review on phase change materials (PCMs) for cold thermal energy storage applications. *Applied Energy*, pp. 513-533.
- Oya, T. et al., 2012. Thermal conductivity enhancement of erythritol as PCM by using graphite and nickel particles. *Applied Thermal Engineering*, p. dx.doi.org/10.1016/j.applthermaleng.2012.05.033.
- Paksoy, H. Ö., 2007. *Thermal Energy Storage for Sustainable Energy Consumption*. s.l.:Springer.
- Palomo, E. & Dauvergne, J.-L., 2011. A non-parametric method for estimating enthalpy-temperature functions of shape-stabilized phase change materials. pp. 1268-1277.
- Pasupathy, A., Velraj, R. & Seeniraj, R., 2008. Phase change material-based building architecture for thermal management in residential and commercial establishments. *Renew. Sust. Energy Rev*, p. 39–64.

PCMProducts, 2009. *Salt Hydrate Based Positive Temperature PCMs*. [Online]

Available at: <http://www.pcmproducts.net/files/PlusICE%20Range-2013.pdf>

[Accessed 1st Jan 2013].

Peck, J., Kim, J., Kang, C. & Hong, H., 2006. A study of accurate latent heat measurement for a PCM with a low melting temperature using T-history method. *International Journal of Refrigeration*, pp. 1225-1232.

Persson M.L, R. A. W. M., 2006. Influence of window size on the energy balance of low energy houses.. *Energy and Buildings*, pp. 181-188.

Pincemin, S., Olives, R., Py, X. & Christ, M., 2008. conductive composites made of phase change materials and graphite for thermal storage. *Sol. Energy Mater. Sol. Cells*, pp. 603-613.

Regin, A., Solanki, S. & Saini, J., 2008. Heat transfer characteristics of thermal energy storage system using PCM capsules: A review. *Renewable and Sustainable Energy Reviews*, pp. 2438-2458.

Rismanchi, B., Saidur, R., BoroumandJazi, G. & Ahmed, S., 2012. Energy, exergy and environmental analysis of cold thermal energy storage (CTES) systems. *Renewable and Sustainable Energy Reviews*, pp. 5741-5746.

Rosiek, S. & Garrido, F., 2012. Performance evaluation of solar-assisted air-conditioning system with chilled water storage (CIESOL building). *Energy Conversion and Management*, pp. 81-92.

Rubitherm, 2012. *Latent heat blend*. [Online]  
Available at: <http://www.rubitherm.de/english/index.htm>  
[Accessed 2013].

Ryu, H. W., Woo, S. W., Shin, B. C. & Kim, S. D., 1992. Prevention of supercooling and stabilization of inorganic salt hydrates as latent heat storage materials. *Sol. Energy Mater. Sol. Cells*, Volume 27, pp. 161-172.

Salunkhe, P. & Shembekar, P., 2012. A review on effect of phase change material encapsulation on the thermal performance of a system. *Renewable and Sustainable Energy Reviews*, pp. 5603-5616.

Salunkhe, P. & Shembekar, P., 2012. A review on effect of phase change material encapsulation on the thermal performance of a system. *Renewable and Sustainable Energy Reviews*, pp. 5603-5616.

- Sandnes, B. & Rekstad, J., 2006. Supercooling salt hydrates: Stored enthalpy as a function of temperature. *Solar Energy*, pp. 616-625.
- Sari, A. & Karaipekli, A., 2007. Thermal conductivity and latent heat thermal energy storage characteristics of paraffin/expanded graphite composite as phase change material.. *Appl. Therm. Eng.*, pp. 1271-1277.
- SEA, 2011. *Energy in Sweden 2011*, s.l.: s.n.
- Shaikh, S. & Lafdi, K., 2006. Effect of multiple phase change materials (pcms) slab configurations on thermal energy storage. *Energy Convers Manage*, p. 2103–2117.
- Sharma, A., Tyagi, V., Chen, C. & Buddhi, D., 2009. Review on thermal energy storage with phase change materials and applications.. *Renewable and Sustainable Energy Reviews*, Volume 13, pp. 318-345.
- Shin, B., Kim, S. & Park, W.-H., 1989. Phase separation and supercooling of a latent heat-storage material. *Energy*, pp. 921-930.
- Siahpush, A., O'Brien, J. & Crepeau, J., 2008. Phase change heat transfer enhancement using copper porous foam. *J Heat Transf*, pp. 082301:1-11.
- Ståhl, F., 2009. *Influence of thermal mass on the heating and cooling demands of a building unit*.. s.l.:Chalmers University of Technology.
- Swedish Energy Agency, 2009. *Energy Indicators*, s.l.: Energimyndigheten.
- Swedish Energy Agency, 2011. *Energy in Sweden*, s.l.: SEA.
- Swedish Tax Office, 2010. *Tax Statistical Yearbook of Sweden 2010*, s.l.: Skatteverket.
- Tay, N., Bruno, F. & Belusko, M., 2013. Comparison of pinned and finned tubes in a phase change thermal energy storage system using CFD. *Applied Energy*, pp. 79-86.
- Teng, Y., 1994. An effective capacity approach to stefan problems using simple isoparametric elements. *International Communications in Heat and Mass Transfer*, p. 179–188.
- Tyagi, V. V. & Buddhi., D., 2007. PCM thermal storage in buildings: A state of art.. *Renew. Sust. Energy Rev.*, Volume 11, p. 1146–1166.
- Verma, N. & Mewes, D., 2009. Lattice Boltzmann methods for simulation of micro and macrotransport in a packed bed of porous

adsorbents under non-isothermal condition. *Computers & Mathematics with Applications*, pp. 1003-1014.

Voller, V., 1990. Fast implicit finite difference method for the analysis of phase change problems. *Numer Heat Transfer*, pp. 155-169.

Voller, V. & Cross, M., 1981. Accurate Solutions of Moving Boundary Problems Using the Enthalpy Method. *Int. J. Heat Mass Transfer*, p. 545–556.

Wang, W. et al., 2009. Enhanced thermal conductivity and thermal performance of form-stable composite phase change materials by using  $\beta$ -Aluminum nitride. *Appl. Energy*, pp. 1196-1200.

Wang, Y. & Yang, Y., 2011. Three-dimensional transient cooling simulations of a portable electronic device using PCM (phase change materials) in multi-fin heat sink. *Energy*, pp. 5214-5224.

White, J., 2005. *Flammability characterization of fat and oil derived phase change materials*. s.l.:University of Missouri-Columbia.

Yin, H., Gao, X., Ding, J. & Zhang, Z., 2008. Experimental research on heat transfer mechanism of heat sink with composite phase change materials.. *Energy Convers. Manage.*, pp. 1740-1746.

Zalba, B., Marín, J. M., Cabeza, L. F. & Mehling, H., 2003. Review on thermal energy storage with phase change: materials, heat transfer analysis and Applications.. *Appl. Therm. Eng.*, pp. 251-283.

Zhang, Y., Jiang, Y. & Jiang, Y., 1999. A simple method , the T -history method , of determining the heat of fusion , specific heat and thermal conductivity of phase-change materials.. *Meas. Sci. Technol.*, Issue 10, pp. 201-205.

Zhao, C., Zhou, D. & Wu, Z., 2011. Heat transfer of phase change materials (PCMs) in porous materials. *Frontiers in Energy*, pp. 174-180.

Zhong, Y. et al., 2010. Heat transfer enhancement of paraffin wax using compressed expanded natural graphite for thermal energy storage. *Carbon*, p. 300–304.